学 位 論 文

Histochemical analysis of a hyarulonan receptor LYVE-1 in the reticulo-endothelial system

（細網内皮系におけるヒアルロン酸受容体 LYVE-1 の組織化学的解析）

2016 年 9 月

北 海 道 大 学

鄭　　淼

Zheng Miao

学 位 論 文

Histochemical analysis of a hyarulonan receptor LYVE-1 in the reticulo-endothelial system

（細網内皮系におけるヒアルロン酸受容体 LYVE-1 の組織化学的解析）

2016 年 9 月

北 海 道 大 学

鄭　　淼

Zheng Miao

Contents

Lists of published papers and presentations

A part of this study was published in the following papers.

1. Miao Zheng, Shunsuke Kimura, Junko Nio-Kobayashi, Hiromi Takahashi-Iwanaga, and Toshihiko Iwanaga

Three types of macrophagic cells in the mesentery of mice with special reference to LYVE-1-immunoreactive cells

Biomed Res 35(1): 37–45, 2014

2. Miao Zheng, Shunsuke Kimura, Junko Nio-Kobayashi, and Toshihiko Iwanaga

The selective distribution of LYVE-1-expressing endothelial cells and reticular cells in the reticulo-endothelial system (RES)

Biomed Res 37(3): 187-198, 2016

A part of this study was presented in the following meetings.

1. Miao Zheng, Toshihiko Iwanaga
   Expression of a monocarboxylate transporter in reticular cells of lymph node and its involvement in uptake of exogenous particles. XXIII International Symposium on Morphological Sciences. Niigata, 10–13 September, 2013
2. Miao Zheng, 木村俊介、小林純子、岩永敏彦
   腸間膜に見られる３種類のマクロファージ様細胞、とくに LYVE-1 陽性細胞
   第 119 回日本解剖学会総会、宇都宮、３月 27~29 日、2014 年
3. Miao Zheng, Toshihiko Iwanaga
   Broad distribution of LYVE-1-expressing endothelial cells and reticular cells with special reference to the reticulo-endothelial system (RES). The 120th Annual meeting of the Japanese Association of Anatomists. Kobe, 21–23 March, 2015
4. Miao Zheng, Toshihiko Iwanaga
   Broad distribution of LYVE-1-expressing endothelial cells and reticular cells with special reference to the reticulo-endothelial system (RES). XXIV International Symposium on Morphological Sciences. Istanbul, 2–6 September, 2015

General introduction

Hyaluronan

Hyaluronic acid (HA), also called hyaluronan, is an anionic, nonsulfated glycosaminoglycan composed of repeating polymeric disaccharides, D-glucuronic acid and N-acetyl-D-glucosamine. It is unique among glycosaminoglycans, since it is directly produced from the plasma membrane instead of the conventional route via Golgi apparatus[1]. As one of the main components of the extracellular matrix, hyaluronan makes a significant contribution to be a key mediator of cell migration, during both embryonic morphogenesis and pathological processes such as wound healing and tumor metastasis[2]. Hyaluronan not only can be found in lower organisms such as simple bacteria, but also in complex eukaryotes. In humans, it is abundantly present in many tissues of the body, including the skin, synovial fluid, skeletal tissues, heart valves, cartilage, vitreous body and so on. The largest amounts are found in the intercellular matrix of skin and musculoskeletal tissues. Hyaluronan is produced and released by many cell types, predominantly mesenchymal cells[2].

Hyaluronan is synthesized by a class of integral membrane proteins called hyaluronan synthases which are present on the inner surface of the plasma membrane[3]. There are three types of hyaluronan synthases: HAS1, HAS2, and HAS3[4,5]. Their main difference is the chain length of the hyaluronan molecules produced by the hyaluronan synthases[6]. The HAS isoforms immediately respond to the environmental changes induced by cytokines or lipopolysaccharide (LPS) and are followed by different control mechanisms. In the previous studies, the expression of HAS1 and HAS2 was found to increase in the lungs

after LPS challenges[7]. The increasing expression of hyaluronan synthases may give another strong demonstration that hyaluronan plays a significant role during inflammation.

Hyaluronan shifts its character depending on its molecular mass; especially, the various fragments stimulate macrophages[8–11] and dendritic cells[12]. In its native form, hyaluronan exists as a high molecular weight polymer which molecular weight reaches the millions such as the normal synovial fluid (>1000 kDa). However, during inflammation and injury, the lower molecular weight fragments (<500 kDa) predominate. The lower molecular hyaluronan fragments were proved to be a key for inducing inflammatory responses in macrophages and dendritic cells[8–11]. Hyaluronidases, a family of enzymes for degrading hyaluronan, show an irreplaceable role for making different mass of hyaluronan. In humans, there are at least six types of hyaluronidase-like enzymes so far: hyaluronidase 1, hyaluronidase 2, hyaluronidase 3, hyaluronidase 4, and hyaluronidase PH-20[13]. They differ in the sides of gene location, tissue distribution, cellular expression, and enzymatic condition. Unlike hyaluronidase 1, hyaluronidase 2 has an effect on high molecular fragments[14]. Unfortunately, other enzymes of the hyaluronidase family are not so clear in functions. The expression of hyaluronidase activities also had been noticed in some diseases such as rheumatoid arthritis, periodontal disease, and scleroderma. An obviously decreased level of serum hyaluronidase 1 was noticed and followed by elevating of circulating hyaluronan. In addition, increased hyaluronan/hyaluronidase production and hyaluronan degradation were detected in injured aorta[15], suggesting that hyaluronan and hyaluronidase production play a crucial role in proliferation and migration of arterial smooth muscle cells.

Most of hyaluronan exists in freely mobilized compartments with a half-life of two days or less, and circulating hyaluronan is mostly derived from lymph[16,17]. About 80–90% of hyaluronan is derived from peripheral lymph before it can reach the bloodstream. Previous studies have confirmed that 10–20% polysaccharide hyaluronan is catabolized locally; more than 80% of tissue hyaluronan is escaped from the local degradation and carried to lymph nodes or the general circulation from where it is cleared by the endothelium of the liver sinusoids[18]. The cell types for uptake and metabolism are primarily endothelial cells of the liver and lymph node which line the sinusoids. In addition, macrophage-like cells are also involved in uptake of hyaluronan in the lymph node and spleen[19].

Hyaluronan receptors

Usually, much of hyaluronan exists as a soluble form in extracellular matrix and binds a variety of proteins which are called hyaluronan receptors to influence the functions. So far, hyaluronan receptors that have been identified as follows: CD44, hyaluronan receptor for endocytosis (HARE), intercellular adhesion molecule (ICAM)-1, RHAMM, LYVE-1, CD34, Toll-like receptors, and so on.

CD44, as a polymorphic type 1 transmembrane glycoprotein, turns out to be the major cell-surface hyaluronan binding protein widely distributed[20]. Most cells including stromal cells—such as fibroblasts and smooth muscle cells—, epithelial cells, and a variety of immune cells express CD44[21]. It can play multiple roles in a variety of biological processes such as development, inflammation, cell recruitment and activation, and tumor growth and

metastasis. HARE (hyaluronan receptor for endocytosis), also termed stabilin-2, has degradation sites and mechanisms different from those of CD44[22]. The degradation by HARE is processed in lysosomes and completes their normal turnover process[19]. HARE is important as a clearance of hyaluronan and chondroitin sulfates from the vascular and lymphatic circulations[19]. Abundant expression of HARE with 175~ and ~300 kDa was detected in the sinusoidal endothelial cells of human liver, lymph node, and spleen[23]. ICAM-1, as a metabolic cell surface receptor for hyaluronan, may be responsible mainly for the clearance of hyaluronan from lymph and blood plasma, which accounts for most of its whole-body turnover[24]. Furthermore, ICAM-1 may also play a role as a cell adhesion molecule, and the HA–ICAM-1 may contribute to the determination of ICAM-1-mediated inflammatory activation[25].

RHAMM is a receptor for HA-mediated motility, also called CD168[26,27]. It is expressed as a functional receptor in many cell types, such as endothelial cells, and alters migratory cell behavior. Extracellularly, RHAMM associates with CD44 and activates intracellular signaling pathways by binding to hyaluronan[28]. Enhanced levels of RHAMM and hyaluronan may be related with the undergoing biochemical failure in patients with prostate cancer[29]. It is also confirmed that once a metastatic lesion has been established, RHAMM can cooperate with CD44 to promote angiogenesis by enhancing migration of neighboring endothelial cells towards the tumor.

LYVE-1 (lymphatic vessel endothelial hyaluronan receptor-1), a 322-residue type 1 transmembrane glycoprotein, has been identified as a reliable marker that is expressed predominantly in the lymphatic endothelium[30]. Then, LYVE-1 has been used for the

detection and isolation of lymphatic endothelial cells. As a receptor for the extracellular matrix hyaluronan, LYVE-1 not only plays a significant role on embryonic and tumour-induced lymphagiogenesis, but also contains a hyaluronan-binding domain to bind and immobilize hyluronan and regulate cell migration[31]. In the previous studies, LYVE-1 has been regarded as a key receptor responsible for the uptake and transport of hyaluronan in the lymph circulation. Thus, LYVE-1 can specifically detect lymphatic vessels in various tissues where the receptor is engaged in the transport of hyaluronan into the vessel lumen. LYVE-1 shares 41% homology with the leukocyte homing receptor CD44 molecule, which supports hyaluronan-mediated rolling on inflamed vascular endothelium. CD44 is widely expressed in the epithelium, mesothelium, mesenchymal cells, and cells of hematopoietic origin, while LYVE-1 has been shown in early studies to display a restricted distribution to the lymphatic endothelium and be completely absent from blood vessels, except for sinusoidal endothelial cells in the spleen[32].

RES and macrophages

The reticulo-endothelial system (RES), originally established by Aschoff in 1924[33], is a cellular system dispersed throughout the body, including macrophages and endothelial cells lining the sinusoids of the liver, lymph nodes, spleen, bone marrow, adrenal gland, and pituitary gland (Table 1). The RES has a higher activity to eliminate circulating exogenous substances and particles such as endotoxins and bacteria. It takes part in formation and destruction of blood cells, storage of fatty materials, metabolism of iron and pigments, and inflammation. However, the concept of RES was historically replaced by the

mononuclear phagocyte system (MPS) with authentic phagocytic activity[34]. The MPS had been defined as a family of cells comprising bone marrow progenitors, blood monocytes and tissue macrophages. However, some studies carried out in the 1990's reconfirmed the fact that RES play an important part of the innate immune system for eliminating foreign particles from the circulation. The researchers used the same vital staining dyes as Aschoff used to demonstrate that endothelial cells in hepatic sinusoids and reticular cells in the lymph node can endocytose them vigorously[35]. Liver sinusoidal endothelial cells are the largest body's reservoir for sinusoidal endothelial cells. Smedsrød and his colleagues[36] have termed the endocytic endothelial cells as scavenger endothelial cells, leading us to resurrect the concept of the RES.

Reticular cells in	Endothelial cells of sinuses in
Splenic red pulp	Lymph node
Medulla of lymph node	Splenic red pulp
	Liver
	Bone marrow
	Adrenal cortex
	Pituitary gland

Table 1 Main members of RES

Macrophages, one of predominant members of RES, play an important role in digesting foreign substances, microbes, and cancer cells. They possess the most intense phagocytic activities among RES members. Broad distribution in the body has been noticed and classified to several types according to the localization, functions,

histochemical/ultrastructural properties, and expression of marker substances[37].

Daems *et al.* have classified macrophages into resident and excudate macrophages based on the subcellular localization of peroxidase[38]. The former is present in consistent sites of normal tissues, while the latter is derived from circulating monocytes and accumulates in inflammatory sites. The resident type contains Kupffer cells, alveolar macrophages, microglia, and so on. These macrophages either are exposed to free spaces of blood vessels and airway or reside in the parenchyme. The connective tissues such as the capsules of organs and interlobular spaces also contain abundant macrophages, which appear to be embedded in collagen fibers. Besides phagocytosis, they also play a critical role in nonspecific defense (innate immunity) and initiate specific defense mechanisms (adaptive immunity) by recruiting other immune cells such as lymphocytes. They are important as antigen presenters to T cells, together with dendritic cells. Recently, based on the functional characteristics and marker substances, macrophages can be further classified to two types: pro-inflammatory M 1 phenotype (classically activated macrophages) or anti-inflammatory M2 phenotype (alternatively activated macrophages)[39], depending on the local environmental stimuli. The M1 stimuli are grouped according to their ability to induce prototypic inflammatory responses and markers. The M2 stimuli are based on the initial Th2 cells (IL-4, IL-13), and their ability to antagonize prototypic inflammatory responses and markers. Membranous tissues such as the omentum and mesentery contain many macrophages and related cells, including Langerhans/dendritic cells. The membranous tissues are very useful for analyzing the whole cell shapes and entire distribution of cells in question. Thus, I focus on macrophagic cells and immunoreactivity

for LYVE-1 in the mesentery (Chapter II).

The present study examined the distribution of LYVE-1-expressing cells at light and electron microscopic levels, focusing on the topographical association with macrophages (Chapter I). I further observed the responses of LYVE-1-expressing cells in LPS-induced inflammation, including the elevated uptake of exogenous particles. In addition, I used a LYVE-1 antibody and macrophage markers to discriminate two types of cells with dendritic processes as well as typical macrophages in the murine mesentery (Chapter II). These cells were observed more clearly and broadly by using whole mount preparations of the mesentery and were compared with macrophages for their shape, distribution, ultrastructure, and uptake ability.

Abbreviations

HA hyaluronan

HARE hyaluronan receptor for endocytosis

ICAM-1 intercellular adhesion molecule-1

LPS lipopolysaccharide

LYVE-1 lymphatic vessel endothelial hyaluronan receptor-1

MPS mononuclear phagocyte system

PBS phosphate buffered saline

RES reticulo-endothelial system

RHAMM receptor for HA mediated motility

RT-PCR reverse transcription-polymerase chain reaction

SSeCKS Src-suppressed-C kinase substrate

TNFα □□□□sforming necrosis factor alpha

Chapter I

The selective distribution of LYVE-1-expressing endothelial cells and reticular cells in the reticulo-endothelial system (RES)

Introduction

LYVE-1 (lymphatic vessel endothelial hyaluronan receptor-1) has been identified as a reliable marker that is expressed predominantly in the lymphatic endothelium[30,40]. Both the chemical structure and function of LYVE-1 resemble those of a well-established hyaluronan receptor, CD44, which has a 41% similarity to LYVE-1 and is characterized as an inflammatory leukocyte homing receptor. CD44 is widely expressed in the epithelium, mesothelium, mesenchymal cells, and cells of hematopoietic origin[41], while LYVE-1 has been shown in early studies to display a restricted distribution to the lymphatic endothelium and be completely absent from blood vessels, except for sinusoidal endothelial cells in the spleen[30]. Subsequent studies have also detected the expression of LYVE-1 in sinusoidal endothelial cells using paraffin sections of the liver, spleen and lymph node of humans[32,42]. However, our preliminary immunohistochemical study using frozen sections from rodents found a broader distribution of LYVE-1 in the endothelium of other organs, including the lung, adrenal gland, heart, and adenohypophysis. In addition, the sinus reticular cells in the medulla of the lymph node intensely expressed LYVE-1. Interestingly, most of these belong to the forgotten concept known as the reticulo-endothelial system (RES).

The RES, originally established by Aschoff in 1924[33,43], was characterized by its higher activity to eliminate circulating exogenous substances and particles such as endotoxins and bacteria. The RES was historically replaced by the mononuclear phagocyte system (MPS) with authentic phagocytic activity by a research group of Van Furth *et al.*[34]: the monocyte-macrophage lineage is the major cell type functioning in the elimination of pathogens and cell-debris, and there is no transition between macrophages and sinusoidal endothelial cells. However, some studies carried out in the 1990's reconfirmed that endothelial cells in hepatic sinusoids and reticular cells in the lymph node

can vigorously incorporate the same vital staining dyes as Aschoff used[35]. It has been shown that endothelial cells—especially hepatic sinusoidal endothelial cells, a representative RES member—comprise an important part of the innate immune system for eliminating foreign particles from the circulation. Smedsrød and his colleagues[36,44,45] have termed the endocytic endothelial cells as scavenger endothelial cells, leading us to resurrect the concept of the RES[46]. A weak point in this effort to re-evaluate the RES is the lack of marker substances that can specify the RES members. In previous studies, we found that Src-Suppressed-C Kinase Substrate (SSeCKS), whose expression was induced by a lipopolysaccaride (LPS) challenge, was shared by some members of RES and was involved in the uptake of exogenous particles[47]. However, the degree of its expression was less intense under normal conditions, and several non-RES cells also expressed SSeCKS[48].

In this chapter I, I examined the distribution of LYVE-1-expressing cells at light and electron microscopic levels, focusing on the topographical association with macrophages. The present study further observed the responses of LYVE-1-expressing cells in LPS-induced inflammation, including the elevated uptake of exogenous particles. The results confirm that LYVE-1 is a key molecule for a reconsideration of the RES concept.

Materials and methods

Animals and tissue sampling. Eight-week-old C57BL/6 and ddY mice of both sexes were used. For conventional microscopic examination, the mice were anesthetized by an intraperitoneal injection with sodium pentobarbital and then perfused with physiological saline through the heart, followed by 4% paraformaldehyde in 0.1 M phosphate buffer, pH 7.4. The liver, lung, spleen, lymph node, heart, adrenal gland, bone marrow, and hypophysis were dissected out and immersed in the same fixative for an additional 8 h. Lipopolysaccharide (LPS, 0.02 mg/20 g body weigh) (E.coli055:B5; Sigma Aldrich, St. Louis, MO) was injected into the peritoneal cavity, and the organs were obtained at 4, 8, 24, and 48 h.

All experiments using animals were performed under protocols following the Guidelines for Animal Experimentation, Hokkaido University Graduate School of Medicine.

Immunohistochemistry. The fixed tissues were dipped in 30% sucrose solution overnight at 4^{o}C, embedded in OCT compound (Sakura Finetek, Tokyo, Japan), and quickly frozen in liquid nitrogen. Frozen sections of 12 μm in thickness were mounted on poly-L-lysine-coated glass slides. After immersion in 0.01 M phosphate buffered saline (PBS) containing 0.3% Triton-X100, the sections were pre-incubated with a normal donkey serum. Sections were incubated with a rabbit anti-mouse LYVE-1 antibody (AngioBio, Del Mar, CA) at a concentration of 1 μg/mL overnight, followed by incubation with Cy3-labeled donkey anti-rabbit IgG (1: 200 in dilution; Jackson ImmunoResearch, West Grove, PA). For double immunofluorescence, sections were stained overnight with a mixture containing the anti-LYVE-1 antibody and rat anti-F4/80 antibody (Clone BM8, 1 μg/mL; BioLegend, San Diego, CA). The sites of antigen-antibody reactions were detected by incubation with a combination of Cy3-labeled anti-rat IgG (1: 200 in dilution; Jackson ImmunoResearch) and AlexaFluor 488-labeled anti-rabbit IgG (1: 100 in dilution; Invitrogen, Carlsbad, CA). Some of the immunostained sections were counterstained

with SyTO 13 (SYTOX, Invitrogen) for observation of the nuclei. Stained sections were mounted with glycerin-PBS and observed under a confocal laser scanning microscope (Fluoview; Olympus, Tokyo, Japan). The specificity of immunoreactions on sections was confirmed according to a conventional procedure, including absorption tests.

Silver-intensified immunogold method for electron microscopy. Frozen sections, 10–14 μm in thickness, were pretreated with normal donkey serum for 30 min, incubated with the rabbit anti-LYVE-1 antibody (1 μg/mL) overnight, and subsequently reacted with goat anti-rabbit IgG covalently linked with 1-nm gold particles (1:200 in dilution; Nanoprobes, Yaphank, NY). Following silver enhancement using a kit (HQ silver; Nanoprobes), the sections were osmicated, dehydrated, and directly embedded in Epon. Ultrathin sections were prepared and stained with an aqueous solution of uranyl acetate and lead citrate for observation under an electron microscope (H-7100; Hitachi, Tokyo, Japan).

In situ hybridization. Two non-overlapping antisense oligonucleotide DNA probes (45 mer in length) were designed for each mRNA of mouse LYVE-1, hyaluronidase 1, and hyaluronidase 2. Antisense probes were complementary to the following sequences: 421–465 and 1331–1375 of *Lyve-1* mRNA (accession number: NM_025989); 1831–1875 and 2651–2695 of *Hyaluronidase 1* mRNA (NM_177568); and 178–222 and 585–629 of *Hyaluronidase 2* mRNA (NM_001081143). The probes were labeled with ^{33}P-dATP using terminal deoxynucleotidyl transferase (Invitrogen). Fresh frozen sections, 14-μm-thick, were fixed with 4% paraformaldehyde in 0.1 M phosphate buffer for 15 min and then acetylated with 0.25% acetic anhydride in 0.1 M triethanolamine-HCl (pH 8.0) for 10 min. Hybridization was performed at 42°C for 10 h with a hybridization buffer containing ^{33}P-dATP-labeled oligonucleotide probes (10,000 cpm/mL). The sections were rinsed at room temperature for 30 min in 2×SSC (1×SSC: 150 mM sodium chloride, 15 mM sodium citrate) containing 0.1% *N*-lauroylsarcosine sodium, then rinsed twice at 55°C for 40 min in 0.1 × SSC containing 0.1% *N*-lauroylsarcosine sodium, dehydrated

through a graded series of ethanol, and air-dried. Sections were exposed to X-ray film (BIOMAX MR Film; Carestream Health, Inc., New York, NY) or dipped in an autoradiographic emulsion (NTB-2; Kodak) at 4°C for 8–10 weeks. The hybridized sections used for autoradiography were counterstained with hematoxylin after development.

The *in situ* hybridization technique using the two non-overlapping antisense probes for each mRNA exhibited identical labeling in all the tissues examined. The specificity of the hybridization was also confirmed by the disappearance of signals upon the addition of an excess of an unlabeled antisense probe.

Non-radioisotope in situ hybridization. Non-isotope *in situ* hybridization was performed with the QuantiGene ViewRNA ISH Tissue Assay (Affymetrix, Santa Clara, CA). The preparation of frozen sections was as described above. Fresh sections were treated with a solution containing 4% paraformaldehyde in PBS for 20 min at room temperature. After three time wash with PBS, the sections were acetylated in 0.1 M triethanolamine (pH 8)/0.25% acetic anhydride for 10 min at room temperature. Subsequent hybridization processes were performed in accordance with the manufacturer's protocol. Specific oligonucleotide probe sets against *Lyve1* (catalog no. VB6-18604) and *Hyal2* (VB1-16724) were purchased from Affymetrix. After hybridization, slides were incubated with Fast Red substrate of alkaline phosphatase for 30 min at room temperature in the dark, rinsed with PBS, and then counter-stained with Gill's hematoxylin.

Quantitative RT-PCR. Total RNA was prepared using TRIzol (Life Technologies) from mouse liver and lung. First-strand cDNA synthesis was completed using ReverTra Ace (TOYOBO, Osaka, Japan). Quantitative PCR reactions were conducted in Rotor Gene 6000 equipment (Qiagen, Hilden, Germany) using KAPA SYBR Green Fast PCR kit (KAPA Biosystems, Woburn, MA). Data were normalized to the expression of glyceraldehyde 3-phosphate dehydrogenase (GAPDH) mRNA. The following primers

were used: *Gapdh*-sense 5'-AGGTCGGTGTGAACGGATTTG-3', *Gapdh*-antisense 5'-TGTAGACCATGTAGTTGAGGTCA-3'; *Lyve1*-sense 5'-CAGCACACTAGCCTGGTGTTA-3', *Lyve1*-antisense 5'-CGCCCATGATTCTGCATGTAGA-3'.

Uptake of exogenous particles. To verify the uptake of exogenous particles by the liver and lung, LPS-treated and control mice were injected directly with fluorescent latex beads, 20 and 100 nm in diameter (Molecular Probes, Eugene, OR) or a physiological saline (control). The animals were anesthetized with halothane gas, and the 0.1 mL of latex bead solution diluted at 1:10 was injected into the inferior vena cava. Ten or 45 min later, the animals were perfusion-fixed under anesthesia, and the liver and lung were removed and immersion-fixed. Frozen sections were immunostained for LYVE-1 as mentioned above.

Results

LYVE-1-expressing endothelial cells and reticular cells

Immunohistochemically, the hepatic sinusoidal endothelium as well as the lymphatics in the interlobular connective tissues stained positively for LYVE-1 in the liver (Fig. 1a), while arterial and venous endothelia were free from any positive immunoreaction. The sinusoidal endothelium in the middle zone of the hepatic lobules displayed a more intense, consistent immunoreactivity than that in the peri-portal and peri-central zones of the lobules. Vascular endothelial cells in the lung (Fig. 1b), the medulla and deep cortex of the adrenal gland (Fig. 1c), the red pulp of the spleen (Fig. 1d), and the atrium of heart (Fig. 1e) were all labeled with the LYVE-1 antibody. In the heart, endothelial cells of the endocardium were intensely immunoreactive, especially in the auricle, while positive staining of the endocardium in the ventricle was restricted to some secluded areas. The mesenteric lymph node possessed immunoreactive reticular cells within sinuses and sinus-lining cells in the medulla (Fig. 1f). These LYVE-1-expressing cells are generally classified as RES for eliminating foreign particles. Although endothelial cells in the pituitary gland and bone marrow have been listed as members of the RES, the pituitary endothelium was free of any LYVE-1 immunoreactivity, but the bone marrow displayed a significant expression in restricted numbers of sinusoidal endothelial cells. The immunostaining results suggest that LYVE-1 presents a novel marker substance for the RES—though not for all members of the RES.

Ultrastructural localization of LYVE-1

The immuno-gold method for electron microscopy labeled the cell membrane of LYVE-1-expressing endothelial cells in the liver (Fig. 2a), lung (Fig. 2b), the medulla of the adrenal gland (Fig. 2c), and spleen. Reticular cells in the lymph node were also heavily immunolabeled (Fig. 2d). The immuno-gold particles for LYVE-1 were localized along the entire length of the plasma membrane in all cell types, while the cytoplasm and nuclei escaped any significant labeling.

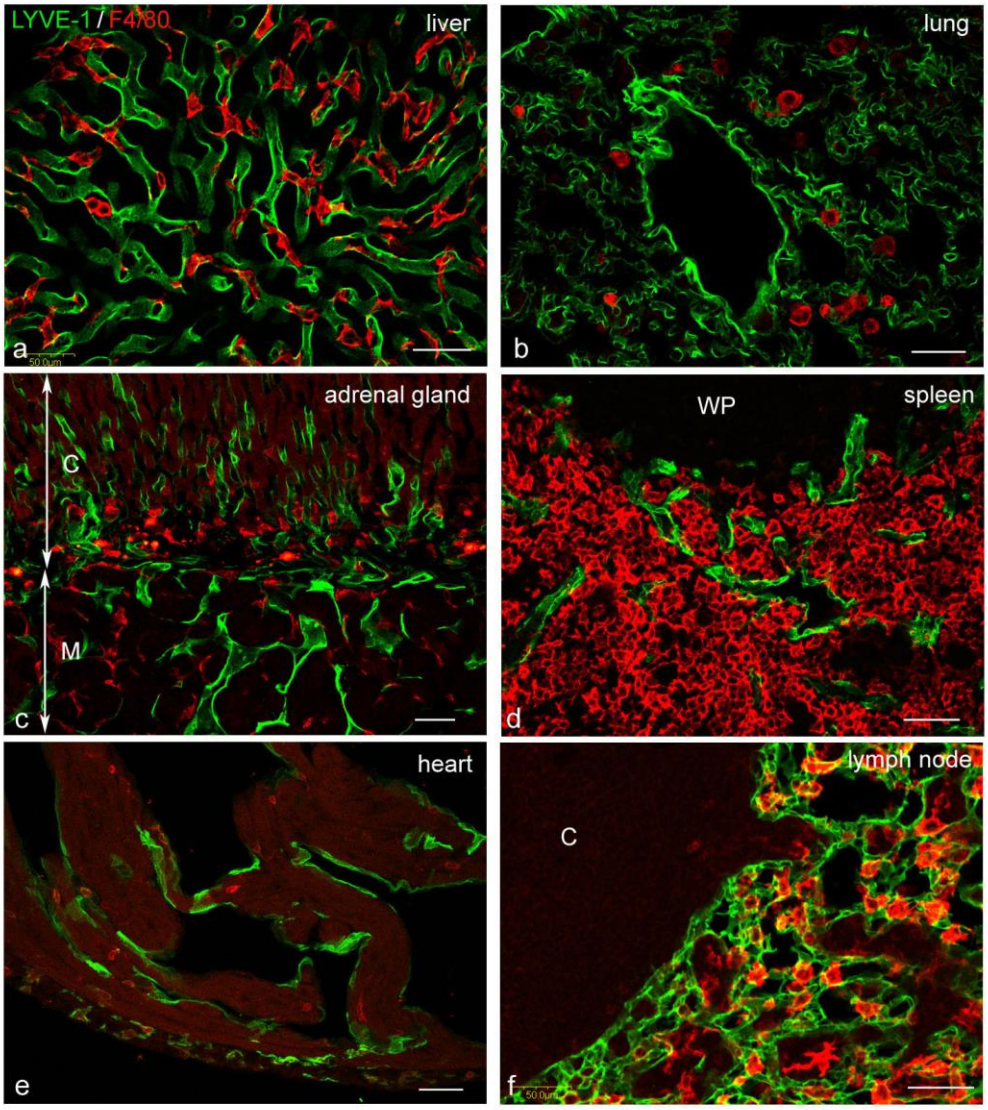

Fig. 1 LYVE-1 immunoreactivities associated with macrophage distribution. Sections were stained with the anti-LYVE-1 antibody (green) and anti-F4/80 antibody (macrophage marker, red). Sinusoidal endothelium of the liver and vascular endothelium of the lung are immunoreactive for LYVE-1, while Kuppfer cells and alveolar macrophages are stained positively for F4/80 (a, b). In the adrenal gland (c), the LYVE-1 antibody labels the vascular endothelium in the medulla and deep cortex. Two-direction arrows indicate the cortex (C) and medulla (M), respectively. In the red pulp of the spleen, LYVE-1-immunoreactive sinuses are embedded in an aggregation of F4/80-positive macrophages (d). The endocardium in the auricle (e) and reticular cells of sinuses in the medulla of lymph node (f) show a positive immunoreactivity for LYVE-1. WP, white pulp; C, cortex *Bars* 50 μm

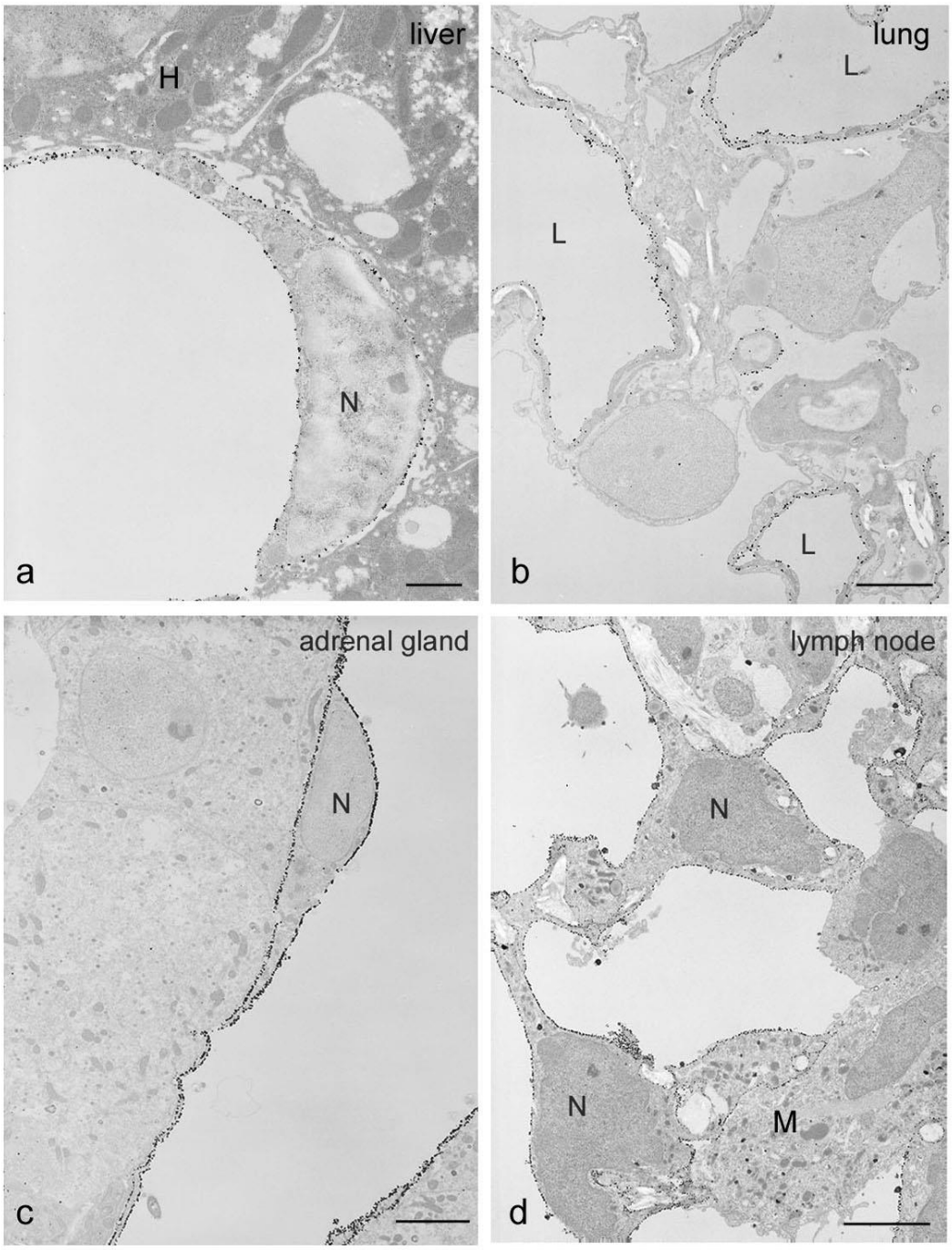

Fig. 2 Immuno-gold method for electron microscopy. Gold particles proving the existence of LYVE-1 are distributed on the luminal and abluminal plasma membrane of endothelial cells in the liver (a), lung (b), and adrenal medulla (c). In the lymph node (d), the cell membranes of reticular cells are immunoreactive along the entire length. H, hepatocyte; L, lumen of lung capillaries; M, macrophage; N, nucleus *Bars* 2 μm (a), 5 μm (b–d)

The LYVE-1-expressing cells are related to macrophages

In light of the LYVE-1 expression in the liver, lung, adrenal gland, spleen, and heart, we examined the relationship between endothelial cells and macrophages at the same regions. Results showed the LYVE-1-immunoreactive endothelial cells to be associated topographically with dense distributions of F4/80$^+$ macrophages, such as Kupffer cells in the hepatic sinusoids (Fig. 1a), alveolar macrophages in the lung (Fig. 1b), macrophages within both the vascular lumen and parenchyma of the adrenal gland (Fig. 1c), macrophages in the red pulp of the spleen (Fig. 1d), and macrophages in the atrium (Fig. 1e). Also in the lymph node, the LYVE-1-immunoreactive reticular cells co-localized with macrophages in the medullary sinuses (Fig. 1f).

Reportedly, some macrophage lineages themselves express LYVE-1. In the chapter II, we found that F4/80$^+$ macrophages in various connective tissues expressed LYVE-1, in contrast to a lack of LYVE-1 in F4/80$^+$ macrophages within the parenchyma of visceral organs. Interestingly, none of macrophage populations mentioned above expressed LYVE-1, for example, macrophages residing in hepatic sinusoids and pulmonary alveoli.

LPS elevates LYVE-1 expression and the uptake activity of latex particles

We hypothesized that the function of LYVE-1-expressing cells may be the uptake and degradation of circulating particles and waste substances including hyaluronan, which is the most abundant glycosaminoglycan in the body and released under normal and pathological conditions. Thus, we first examined the uptake ability of LYVE-1-expressing cells. Since the uptake of fluorescent latex beads intravenously injected was scanty in the LYVE-1-expressing cells under normal conditions, we tried to stimulate LYVE-1-expressing cells by LPS injection into the peritoneal cavity of mice.

When we analyzed the mRNA expression of LYVE-1 by a quantitative RT-PCR in mice, the exposure to LPS for 4 h caused about a four fold increase in the LYVE-1 mRNA expression of the liver as compared with control livers (Fig. 3). In the lung, LPS administration also caused a significant increase in LYVE-1 at 4 h. The expression levels

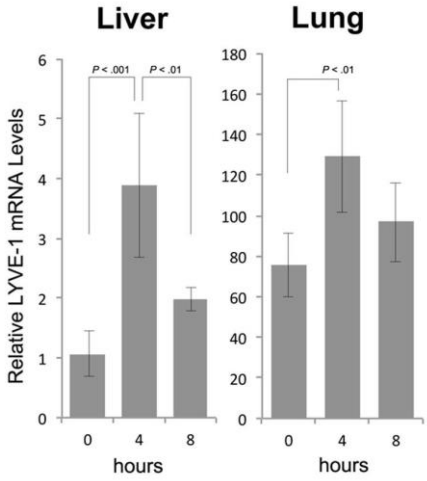

Fig. 3

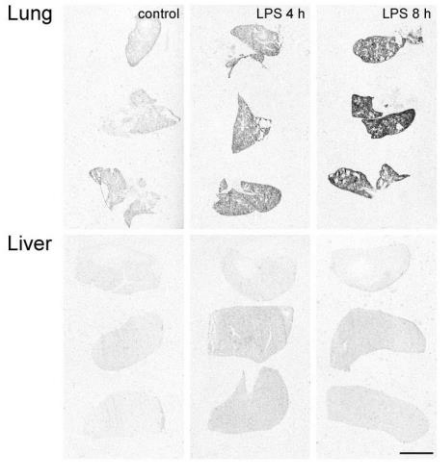

Fig. 4

Fig. 3 Measurement of mRNA using quantitative RT-PCR shows the changes in LYVE-1 mRNA expression after an LPS administration. The expression peaked at 4 h after the administration in both the liver and lung. Value at 0 h in the liver is set at 1 in the figure.

Fig. 4 *In situ* hybridization analysis for LYVE-1 mRNA expression after LPS administration. Sections from the lung (upper panels) and liver (lower panels) of three animals at each time point (0, 4, and 8 h after LPS) were hybridized and exposed on an X-ray film. The expression of LYVE-1 mRNA in the lung increases in intensity with time following the LPS challenge. The liver shows a slight increase in mRNA expression in two of the three animals. *Bar* 5 mm

of LYVE-1 mRNA in these organs tended to decrease after 8 h but was still higher than the controls. X-ray film images of an *in situ* hybridization method confirmed elevated expressions of LYVE-1 mRNA at 4 h and 8 h after the LPS challenge in the lung (Fig. 4). There was a slight but significant change in LYVE-1 signals in the liver between LPS-injected mice and control mice. In accordance, the LYVE-1 immunoreactivity in the endothelial cells of the liver and lung increased in intensity at 24 and 48 h after the LPS challenge; longer exposure to LPS induced a more intense expression at a protein level (Fig. 5). There were no remarkable changes in the density or intensity of LYVE-1

immunoreactivity after the LPS injection in other tissues such as the spleen, heart, and adrenal gland (data not shown).

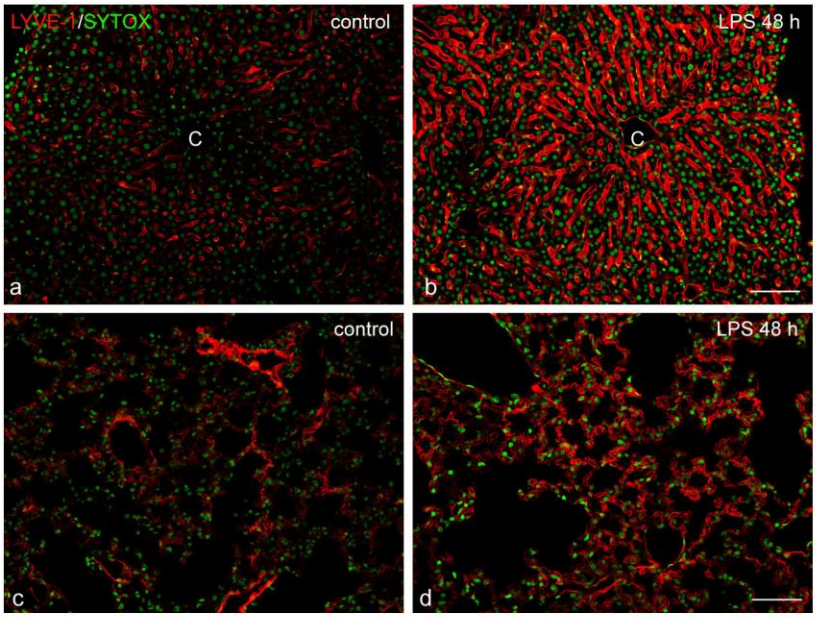

Fig. 5 LYVE-1 immunoreactivities in controls and at 48 h after LPS administration. LPS stimulation elevates the LYVE-1 immunoreactivities in the vascular endothelium of the liver (a, b) and lung (c, d). Nuclei are stained with SYTOX green. C, central vein *Bars* 100 μm

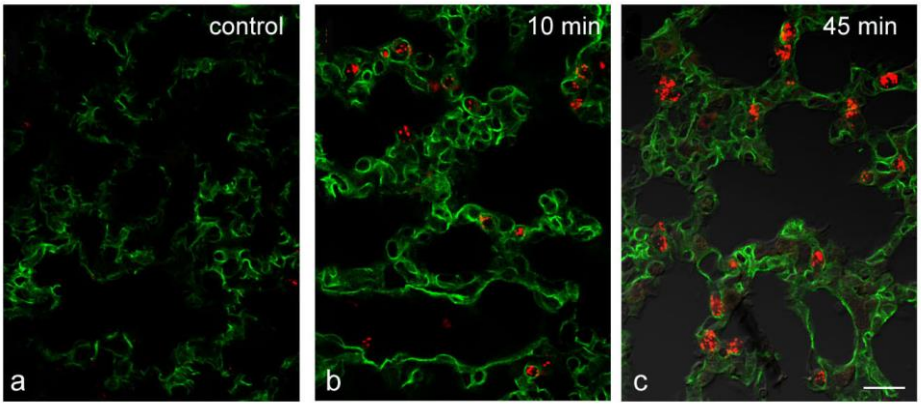

Fig. 6 Uptake of 20 nm fluorescent latex particles in the lung capillaries. The endothelium does not uptake latex particles under the control (a). When the animals were stimulated by LPS for 24 h, the capillary endothelium captures some red latex particles 10 min after administration (b) and many particles 45 min after administration (c). LYVE-1 immunoreactivity is seen green. *Bars* 20 μm

Next, the uptake of exogenous substances in the lung was examined by fluorescent latex beads of 20 nm and 100 nm in diameter being injected directly into the inferior vena cava (Fig. 6). In normal conditions, some alveolar macrophages slightly incorporated the latex particles of 20 nm, while no significant uptake was visible in the endothelial cells of lung capillaries. The LPS challenge induced the trapping and uptake of abundant 20-nm latex particles by endothelial cells at 24 h. Latex particles appeared in the capillary wall at 10 min after the intravenous injection of particles and increased in number at 45 min (Fig. 6). However, large latex particles, 100 nm in size, accumulated only in macrophages but were not incorporated by endothelial cells, even in LPS-stimulated mice (data not shown).

Finally, we examined the activity for degrading hyaluronan by detecting hyaluronidases in murine tissues. Due to the lack of available antibodies against hyaluronindases, we tried to detect these enzymes by an *in situ* hybridization technique using ^{33}P-labeled DNA probes. We checked two major types of hyaluronidases: hyaluronidases 1 and 2[49]. Since these hyaluronidases showed the same expression pattern, we shall describe hyaluronidase 2 as a representative example. X-ray film images detected a significant expression of hyaluronidase 2 mRNA in the lymph node, liver, and lung with various intensities, in addition to the kidney and small intestine under normal conditions. Because of the most intense expression of hyaluronidase 2 mRNA in the medulla of the lymph node, we compared the detailed expression pattern with that of LYVE-1 mRNA in this region. Both signals were concentrated in the medullary sinuses, but they did not appear to correlate at cellular levels. The non-radioisotope *in situ* hybridization method further demonstrated that macrophages of large cell bodies expressed hyaluronidase 2 mRNA (Fig. 7a), in contrast to the LYVE-1 mRNA expression that was restricted to reticular cells with a scanty cytoplasm (Fig. 7b). Noteworthy, reticular cells with LYVE-1 mRNA expression were frequently in direct contact with macrophages expressing hyaluronidase 2 mRNA, as shown in the same sections (Fig. 7 c, d).

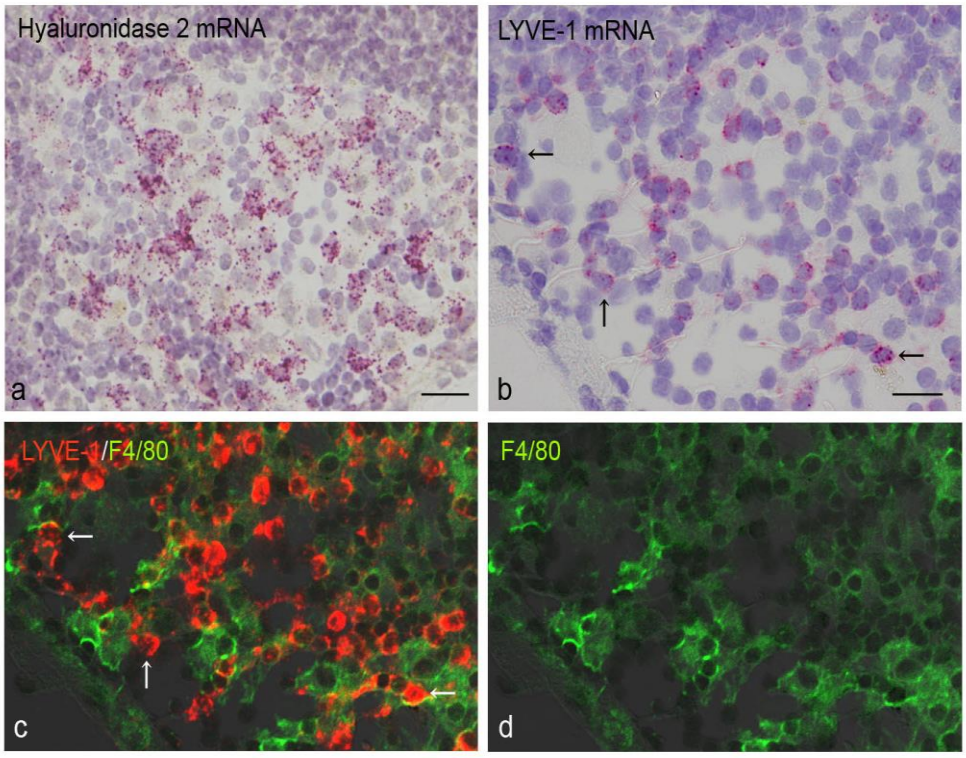

Fig. 7 *In situ* hybridization analysis of hyaluronidase 2 and LYVE-1 mRNAs in the medulla of the lymph node. Signals for hyaluronidase 2 mRNA are seen in large cells with a rich cytoplasm and pale nucleus (a), while those for LYVE-1 mRNA are restricted to cells with a scanty cytoplasm (arrows in b). Counter-staining with hematoxylin. The same section as Fig. b was stained for F4/80, and observed under a confocal microscope for the dual detection of LYVE-1 mRNA and F4/80 immunoreaction (c, d). Arrows in b and c indicate the same reticular cells. *Bars* 20

Discussion

The present study using mice revealed an extensive distribution of "lymphatics-dominant" LYVE-1 in the endothelium of several blood vessels as well as the sinusoidal endothelium of the liver and spleen. Ultrastructually, LYVE-1 was localized at the plasma membrane of these endothelial cells on both luminal and abluminal (basal) sides. An LPS challenge induced a significant up-regulation of LYVE-1 expression in lung capillaries and hepatic sinusoids, with a concomitant elevation of uptake ability for 20 nm-latex particles. Since a predominant localization of hyaluronidases was restricted to adjacent macrophages, the degradation of hyaluronan may be completed in the relay of macrophages.

LYVE-1 is a novel marker for the reticulo-endothelial system (RES)

LYVE-1 has been believed to be a hyaluronan receptor molecule abundantly expressed in the endothelium of lymphatic vessels, with additional expressions in sinusoidal endothelia of the liver, lymph node, and spleen and in some macrophage lineages[32,42,50–52]. However, we found a broader distribution of LYVE-1: vascular endothelial cells in the lung, adrenal gland, and endocardium. The present report is the first study using cryostat sections to detect LYVE-1 in the non-sinusoidal vascular endothelial cells. Interestingly, Gordon *et al.*[53] have documented positive staining for LYVE-1 in the cardiac endothelium and lung capillaries of mouse embryos, though they considered this reactivity an indicator of immature vessels. The sinus reticular cells as well as sinus-lining endothelium (especially medulla) of the lymph node also expressed LYVE-1, in agreement with previous studies in the human lymph node[42]. In contrast to the reported positive staining of LYVE-1, Mouta Carreira *et al.*[32] failed to immunolabel the endothelium of splenic sinusoids in mouse strains. This failure may be explained partially by differences in strain species and sex in the immunoreactivity for LYVE-1, as we have experienced. The LYVE-1-expressing cells shown in the present study are largely classified as members of a previously-held concept, the RES[43,54]. Although the sinusoidal endothelial cells of the pituitary gland, nominated as a member of the RES, lacked the LYVE-1 immunoreactivity in the mouse,

the pituitary gland of rats contained many LYVE-1-immunoreactive endothelial cells. The cellular distribution of LYVE-1 differs from that of another hyaluronan receptor molecule, CD44, which is absent in vascular endothelial cells but mainly localized in several types of epithelia and immune cells such as lymphocytes and macrophages[41]. Stabilin-2 functions as an endocytic receptor removing hyaluronan from the blood[55,56]. Immunohistochemically, stabilin-2 is distributed in not only the sinusoidal endothelium of the liver, lymph node, spleen, and bone marrow, but also the epithelia of several organs[57]. Our previous study demonstrated the selective up-regulation of Src-Suppressed-C Kinase Substrate (SSeCKS) by an LPS challenge in several RES members, including endothelial cells of the liver, lung, spleen, and pituitary gland[48]. Unlike LYVE-1, the expression levels of SSeCKS were so low that its immunoreactivity in the endothelial cells of RES was undetectable under normal conditions. Thus, LYVE-1 shared by vascular endothelial cells, reticular cells, and macrophages may be a more reliable and specific marker substance of the RES, even under normal conditions.

Uptake of exogenous substances by LYVE-1-expressing cells

LYVE-1 was initially regarded a key receptor responsible for the uptake and transport of hyaluronan in the lymph circulation[30,40]. However, subsequent studies using knock-out mice have revealed that the expression of LYVE-1 in the lymphatic vessels is dispensable for both the hyaluronan metabolism and leukocyte trafficking[58]. The lack of significant alternations in hyaluronan homeostasis was explained by functional masking or silencing by a mechanism of sialylation, and the hidden functions might be released by a cytokine-stimulated membrane-bound sialidase activity[59]. These findings led researchers to speculate that a critical function of the receptor might only appear under stress conditions such as inflammation, especially during early stages. Unexpectedly, pro-inflammatory cytokines such as TNFs induced the rapid internalization and subsequent degradation of LYVE-1 itself *in vitro*, and TNF-mediated inflammation markedly reduced the staining of LYVE-1 in lymphatic vessels *in vivo*[60]. Also, macrophages tended to show

a similar response under systemic inflammation induced by LPS[52]. In contrast, the present study showed that LPS stimulation conversely increased the expression of LYVE-1 in the endothelial cells of the liver and lung, as demonstrated by quantitative RT-PCR and immunostaining. This means that the regulation of LYVE-1 expression—possibly also the functions—differ between lymphatics and blood vessels. In accordance with the elevated expression of LYVE-1, the uptake of latex beads was up-regulated by LPS in the endothelium of lung capillaries. Although the present study did not examine the endocytosis of hyaluronan-conjugated particles, studies concerning the drug delivery system focus on the effective uptake of hyaluronan-decorated particles by cancer cells which overexpress CD44, a LYVE-1 homologue[61,62]; the uptake of hyaluronan-conjugated platinum particles by carcinoma cells was about 50% lower with pre-treatment with the anti-CD44 antibody[63].

Modern methodology—including electron microscopic observation—has denied any phagocytotic activity in the RES except for macrophages. However, accumulating evidence has reconfirmed the uptake of denatured proteins, vital staining dyes, and small particles by the hepatic sinusoidal endothelium and lymph node reticular cells[35,47]. It is generally accepted that hepatic sinusoidal endothelial cells play a pivotal role in the clearance of blood-born waste macromolecules and particles by receptor-mediated endocytosis, whereas large particles are phagocytosed by Kupffer cells[45]. Most researchers have not paid attention to the uptake of exogenous particles in the endothelium of the lung, adrenal gland, and heart, where we demonstrated the selective expression of LYVE-1 in the present study. However, historical studies have documented the uptake of proteins and particles in these organs: sinus endothelial cells of the adrenal gland were able to ingest denatured serum proteins[64,65]. The vascular endothelial cells of the rat adrenal gland were able to uptake ferritin from the blood stream, and the ferritin particles easily penetrated into the subendothelial spaces[66]. The bone marrow sinusoidal endothelial cells endocytosed modified serum albumin in mice, rats, and rabbits[64,65,67]. Information concerning the cardiac endothelium is limited regarding the uptake of circulating

substances. The endocardial endothelial cells of fish have been shown morphologically to endocytose vigorously labeled collagen and hyaluronan; the uptake ability was higher in the atrium than in the ventricle[68,69]. Thus, the vascular endothelial cells of the RES serve as the most important site for the elimination of waste products and small particles in circulation, while macrophages including Kupffer cells may play a minor part in the clearance of them circulating in the blood.

Topographical and functional relationship between LYVE-1-expressing cells and macrophages

Hyaluronan, a large glycosaminoglycan with molecular weights reaching the millions, is abundantly present as an extracellular matrix component. Tissue hyaluronan that has escaped from local metabolism enters lymphatic vessels and is transported to the lymph nodes, where as much as 80–90% of hyaluronan is degraded[1,70]. This finding is supported by the most intense expression of hyaluronidase mRNA appearing in the lymph node, as demonstrated by the present study. A small part of hyaluronan and/or fragments enter the blood circulation and are processed mainly in the hepatic sinusoidal endothelial cells[71]. Accordingly, the LYVE-1 of the lymphatic endothelium was initially regarded a key receptor responsible for the uptake and transport of hyaluronan in tissues and lymph circulation. However, subsequent studies using knock-out mice showed that the expression of LYVE-1 in the lymphatic endothelium is not essential for the hyaluronan metabolism, as mentioned above. Stabilin-2 (also termed HARE) is considered the main receptor for endocytosis of hyaluronan, heparin, and chondroitin sulfates in the hepatic sinusoidal endothelium[55,72]. Although LYVE-1 may play an important role in the uptake of hyaluronan in the lymph nodes, stabilin-2 rather than LYVE-1 appears to be the primary receptor for lymphatic degradation[40].

Information on the cellular expression of the hyaluronan degrading enzymes is important for identification of the degradation sites. We confirmed the accumulated expression of hyaluronidases in the medulla of lymph node. Noteworthy, the expression

of hyaluronidases there was restricted to macrophages but not reticular cells. Ultrastructually, LYVE-1 is always localized in the plasma membrane but not in the cytoplasm and cell organelle, in contrast to its cytoplasmic localization in macrophagic cells, such as intracellular vesicles and vacuoles[51,52]. The dual membrane localization of LYVE-1 in the vascular endothelial cells is in agreement with early observations concerning LYVE-1 in the endothelium of lymphatics[40], suggesting transport via the cells (transcytosis) without intracellular degradation.

Our immunohistochemical data showed that the LYVE-1-immunoreactive cells were topographically associated with a dense distribution of macrophages in each tissue: Kupffer cells in the hepatic sinusoids, alveolar macrophages in the lung, macrophages within both sinusoidal lumen and parenchyma of the adrenal gland, macrophages in the splenic red pulp, and macrophages in the auricular wall. Electron microscopy suggested that the phagocytosis of circulating particles in the adrenal gland and adenohypophysis was accomplished by the perivascular macrophages with processes passing through endothelial cells and extending into the lumen of the vessels[73]. In the lymph node, we were able to visualize the intimate relation of reticular cells with hyaluronidase-expressing macrophages. Taken together, these findings give credence to the notion that the LYVE-1-expressing RES cells may capture circulating hyaluronate and process it with relation to adjacent macrophages with intense hyaluronidase activities.

In conclusion, LYVE-1 is important for an evaluation of the RES as well as a marker substance, leading us to the resurrection of the RES. LYVE-1 expressed in the RES, especially in the vascular endothelium, may have different functions from that in lymphatic vessels.

Chapter I I

Three types of macrophagic cells in the mesentery of mice with special reference to LYVE-1-immunoreactive cells

Introduction

Membranous tissues such as the omentum and mesentery contain many macrophages and related cells, including Langerhans/dendritic cells. However, their distinct classification and functions remain unclear. As shown by their stainability with marker antibodies and enzymatic activities, cells with dendritic morphology in the rat omentum were very close to Ia antigen-positive interdigitating cells of lymphatic tissues[74]. This study also noted that cells with dendritic morphology in the rat omentum were fairly heterogeneous[74]. Zhu *et al.*[75] recognized the stellate or dendritic cells in the mouse omentum to be scavenging macrophages due to their phagocytic activity, stainability to marker antibodies, and severe reduction in number in *op/op* mice which lack the macrophage colony-stimulating factor (M-CSF). The omental dendritic cells are slender or stellate in shape, projecting long cytoplasmic processes, while typical macrophages are round in shape. Furthermore, the dendritic cells are embedded in the connective tissue of the omentum, in contrast to round macrophages being exposed to the peritoneal cavity. The somewhat confusing classification and terminology of cells with dendritic morphology in the omentum may be partially due to the use of different marker antibodies and sampling under different conditions. Since macrophages or dendritic cells in membranous tissues facing the peritoneal cavity have quite a large population and play an important role in homeostasis of the peritoneal cavity, they should be classified more exactly as they are related to their diverse functions.

LYVE-1 is a transmembrane glycoprotein that contains a hyaluronan-binding domain to bind and immobilize this common extracellular matrix molecule[30,40]. Hyaluronan undergoes rapid turnover with a half-life of ~24 h, and more than 80% of tissue hyaluronan is degraded within the lymph nodes[70,71,76]. Immunohistochemistry for LYVE-1 can

specifically detect lymphatic vessels in various tissues where the receptor is engaged in the transport of hyaluronan into the vessel lumen[40]. LYVE-1 had been regarded a key receptor responsible for the uptake and transport of hyaluronan in the lymph circulation. Besides lymphatic endothelial cells, the hepatic sinusoidal endothelium and some populations of macrophages express LYVE-1[32,77]. As described in chapter I, macrophages are important members of RES. LYVE-1 is expressed in typical $CD11b^+$, $F4/80^+$ macrophages in peri-tumour connective tissue, and in wound healing tissues of mice[78]. Another LYVE-1 immunoreactivity is found in human fetal macrophages within the chorion villi of the placenta[79] as well as in the murine fetal macrophages in the developing kidney[51]. The expression of LYVE-1 by macrophages suggests functions other than the transport of tissue hyaluronan into lymph circulation: *1)* the uptake and degradation of hyaluronan, *2)* cell adhesion and migration in the extracellular matrix, and *3)* regulation of inflammation. Our preliminary study of the murine mesentery using an antibody against LYVE-1 stained a great number of specialized cells which possessed long processes, were distributed in equal spaces, but differed from $F4/80^+$ typical macrophages.

The present immunohistochemical study using a LYVE-1 antibody and macrophage markers discriminates two types of cells with dendritic processes as well as typical macrophages in the murine mesentery. These cells were observed more clearly and broadly by using whole mount preparations of the mesentery and were compared with macrophages for their shape, distribution, ultrastructure, and uptake ability.

Materials and methods

Tissue samples of mesentery. Adult female ddY mice, weighing about 25–28 g, were used in this study. The mice were sacrificed by bloodletting from the heart under deep anesthesia with pentobarbital sodium. Pieces of fresh mesentery tissues were collected, mounted as a sheet on glass slides, and air-dried. Lipopolysaccharide (LPS, 0.02 mg/20g body weigh) (E. coli 055:B5, Sigma Aldrich) was injected into the peritoneal cavity, and the mesentery was obtained at 1 and 2 days after the injection (*n*=3 for each time point). Latex particles of 20 nm in diameter (FluoSpheres, carboxylate-modified, red [580/605]; Life Technologies, Eugene, OR) were injected into the peritoneal cavity at a dose of 100 μL diluted by 400 μL saline, and the mesentery was obtained 3 h, 1 day, and 2 days after injection (*n*=3 for each time point). All experiments using animals were performed under protocols following the Guidelines for Animal Experimentation, Hokkaido University Graduate School of Medicine.

Using the whole mount preparations mentioned above, fixation was done with 10% formalin in 0.1 M phosphate buffer (pH 7.4) for 2 h. The specimens were then immersed in 0.01 M phosphate buffered saline (PBS) containing 0.3% Triton-X100 for 1 h to enhance the penetration of antibodies and in 100% ethanol for 30 min to remove lipid from the samples.

For conventional immunohistochemistry using cryostat sections, another five mice were perfused with a physiological saline through the heart under deep anesthesia, followed with 4% paraformaldehyde in 0.1 M phosphate buffer. The liver, lymph node, thymus, spleen, interscapular brown adipose tissue, ovary, kidney, adrenal gland, brain, and mesentery were dissected out and immersed in the same fixative for an additional 6 h. The fixed tissues were dipped in 30% sucrose overnight at 4℃, embedded in OCT compound (Sakura FineTechnical Co. Ltd., Tokyo, Japan), and quickly frozen in liquid nitrogen. Frozen sections of a 10 μm thickness were mounted onto poly-L-lysine-coated glass slides and immersed in PBS containing 0.3% Triton-X100 for 1 h.

Immunohistochemistry of LYVE-1 and F4/80. Cryostat sections on glass slides were pretreated with 0.03% H_2O_2 in methanol to block the endogenous peroxidase activity. They were further pretreated with a normal goat serum and incubated with a rabbit anti-mouse LYVE-1 antibody (AngioBio, Del Mar, CA) at a concentration of 1 μg/mL overnight. The sites of the antigen-antibody reaction were detected by incubation with biotin-conjugated goat anti-rabbit IgG (Nichirei, Tokyo, Japan), followed by incubation with the avidin-peroxidase complex (Vectastain ABC kit; Vector, Burlimgame, CA). The reactions were visualized by incubation in 0.05 M Tris-HCl buffer (pH 7.6) containing 0.01% 3,3'-diaminobenzidine and 0.001% H_2O_2.

For immunofluorescence, samples were pretreated with normal donkey serum and incubated with a rabbit anti-LYVE-1 antibody (2 μg/mL) overnight, followed by incubation with Cy3-labeled anti-rabbit IgG (1:200 in dilution; Jackson ImmunoResearch, West Grove, PA). For double immunofluorescence of whole mount preparations and tissue sections, the samples were pretreated with normal donkey serum and incubated with a mixture of rabbit anti-LYVE-1 antibody (2 μg/mL) and rat anti-F4/80 (Clone CI:A3-1 or BM8, 1 μg/mL; BioLegend, San Diego, CA) overnight. The sites of the antigen-antibody reaction were detected by incubation for 2 h with Cy3-labeled anti-rat IgG (Jackson ImmunoResearch) and AlexaFluor 488-labeled anti-rabbit IgG (Invitrogen, Carlsbad, CA). Stained samples were mounted with glycerin-PBS and observed under a confocal laser scanning microscope (Fluoview; Olympus, Tokyo, Japan). Some of immunostained sections were counterstained with SyTO 13 (Invitrogen) for observation of the nuclei.

Immunoelectron microscopy. We used two different methods for electron microscopic observation of LYVE-1-immunoreactive cells in the mesentery. After blocking the endogenous peroxidase activity, paraformaldehyde-fixed cryostat sections were pretreated with normal goat serum for 1 h and incubated with the rabbit anti-LYVE-1 antibody (1 μg/mL) overnight. Following washing, they were incubated with peroxidase-labeled anti-rabbit IgG (Dako Japan, Tokyo) for 3 h. The antigen-antibody reactions were

detected by incubation in 0.05 M Tris-HCl buffer (pH 7.6) containing 0.01% 3,3'-diaminobenzidine and 0.001% H_2O_2, and post-fixed in 1% OsO_4 for 30 min. The specimens were dehydrated through a graded series of ethanol and directly embedded in Epon (Nisshin EM, Tokyo, Japan).

The silver-intensified immunogold method is described in Chapter I.

Results

Immunohistochemistry of LYVE-1 and F4/80 in mesentery

Observation of whole mount preparations of the mesentery revealed the entire shape and distribution of LYVE-1-immunoreactive cells (LYVE-1^+ cells). Intensely immunoreactive cells for LIVE-1 were evenly distributed throughout the mesentery and projected thick processes (Fig. 8a). They usually projected two or three processes which extended in opposite or triangular directions (Fig. 8c, e). We have tentatively termed these cells as Type 1 LYVE-1^+ cells. Another type of LYVE-1^+ cell, termed as Type 2 LYVE-1^+ cells, was characterized by an irregular cell surface and shaggy contours with the tufty fine processes shown in Figures 8b, c, and f. In observations of cryostat sections, both types of LYVE-1^+ cells appeared to be wholly embedded in membranous tissues of the mesentery (Fig. 8d). These two types of LYVE-1^+ cells were weakly or moderately positive for F4/80, a marker of murine macrophages, as compared to round macrophages with an intense labeling (Fig. 9a, b). Interestingly, two types of LYVE-1^+ cells were segregated, possessing their own territory of distribution (Fig. 8c). Immunohistochemistry using the F4/80 antibody detected typical round macrophages with uneven distribution: they often aggregated in some places of the mesentery (Fig. 9a, b). These macrophages were absolutely negative in reaction for LYVE-1. Immunostaining of CD11c, a marker of dendritic cells, failed to stain both LYVE-1^+ cells with dendritic morphology and F4/80^+ macrophages (data not shown).

Uptake of exogenous particles

When fluorescent latex particles of 20 nm in diameter were injected into the peritoneal cavity, only F4/80^+ macrophages vigorously ingested the latex particles at 3 h after the injection; no LYVE-1^+ cells contained latex particles in their cytoplasm (Fig. 9c). However, a moderate uptake of latex particles by LYVE-1^+ cells was found at 1 or 2 days after the injection (data not shown).

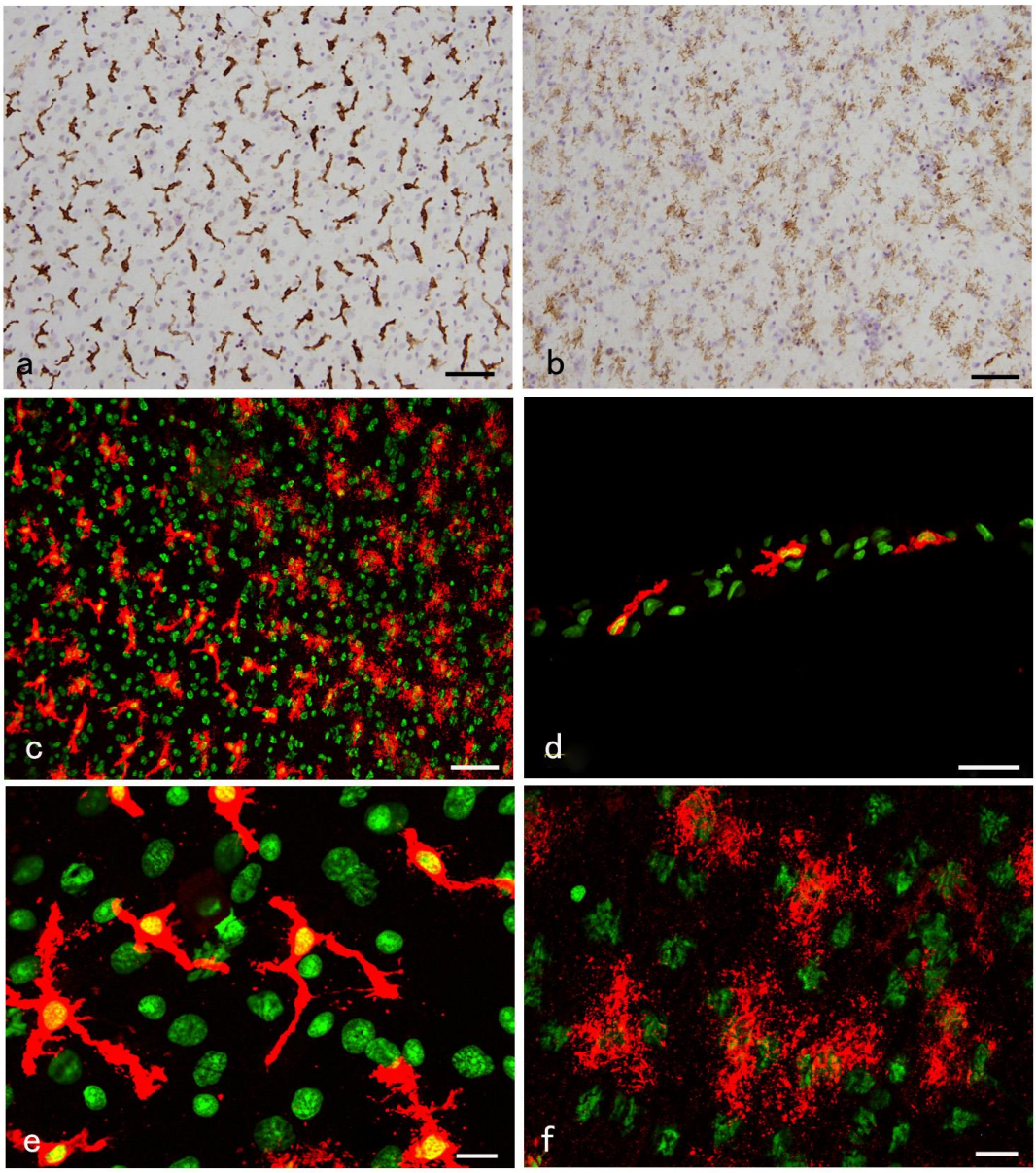

Fig. 8 Two types of LYVE-1-immunoreactive cells in the murine mesentery, shown by the ABC method (a, b, nuclear staining with hematoxylin) and immunofluorescence method (c–f, nuclear staining with green fluorescein). Intensely positive slender or dendritic cells (a) and moderately immunoreactive cells (b) are evenly distributed at regular intervals. These two types of LYVE-1$^+$ cells have their own territory on the right and left sides of picture. Observation of a tissue section shows LYVE-1$^+$ cells localized within the membranous tissue of the mesentery. A closer view demonstrates the detailed morphology of LYVE-1$^+$ cells (Type 1 cells in e; Type 2 cells in f). In figures c–f, nuclei are stained green by SyTO. Bars: 100 μm (a, b), 50 μm (c, d), 20 μm (e, f)

Response to inflammation induced by LPS

Injection of LPS into the peritoneal cavity induced dynamic changes in LYVE-1$^+$ cells of the mesentery. At 1 and 2 days after the LPS challenge, most of the LYVE-1$^+$ cells had lost the immunoreactivity to the LYVE-1 antibody and come to be more intensely immunoreactive for F4/80 as compared with normal conditions (Fig. 9d). Also, two types of LYVE-1$^+$ cells, now visualized only by the F4/80 antibody, changed their morphology (Fig. 9e, f). Especially, Type 1 LYVE-1$^+$ cells elongated to extend long and slender processes in many directions, similar to astroglia in the brain (Fig. 9e).

Ultrastructure

LYVE-1-positive cells within the mesentery were identified by a heavy labeling of osmium black under the electron microscope (Fig. 10a). The LYVE-1$^+$ cells contained vesicles of various sizes as well as rough endoplasmic reticulum and Golgi apparatus. By the immunogold method, LYVE-1$^+$ cells in whole mount preparations were heavily labeled with gold particles (Fig. 10b). LYVE-1$^+$ cells displayed complicated contours and were embedded by collagen fibrils. The LYVE-1 immunoreactivity detected by the two methods was found throughout the cell bodies but were more intense near the plasma membrane.

LYVE-1 immunoreactivity in macrophages of other organs

In contrast to mesentery F4/80$^+$ macrophages, F4/80$^+$ macrophages dispersed in various connective tissues intensely expressed LYVE-1. In the joint, macrophages in the synovial membrane (type A synoviocytes) and in the deeper region of the synovium were immunoreactive for both LYVE-1 and F4/80 (data not shown). The capsules and interstitium of the kidney (Fig. 11a), brown adipose tissue, thymus, and lymph node contained LYVE-1$^+$ F4/80$^+$ cells. Although F4/80$^+$ cells were rich in the parenchyma of these organs, they were absolutely free from LYVE-1 immunoreactivity. Brain F4/80$^+$ macrophages (microglia) were not immunoreactive for LYVE-1, and only F4/80$^+$

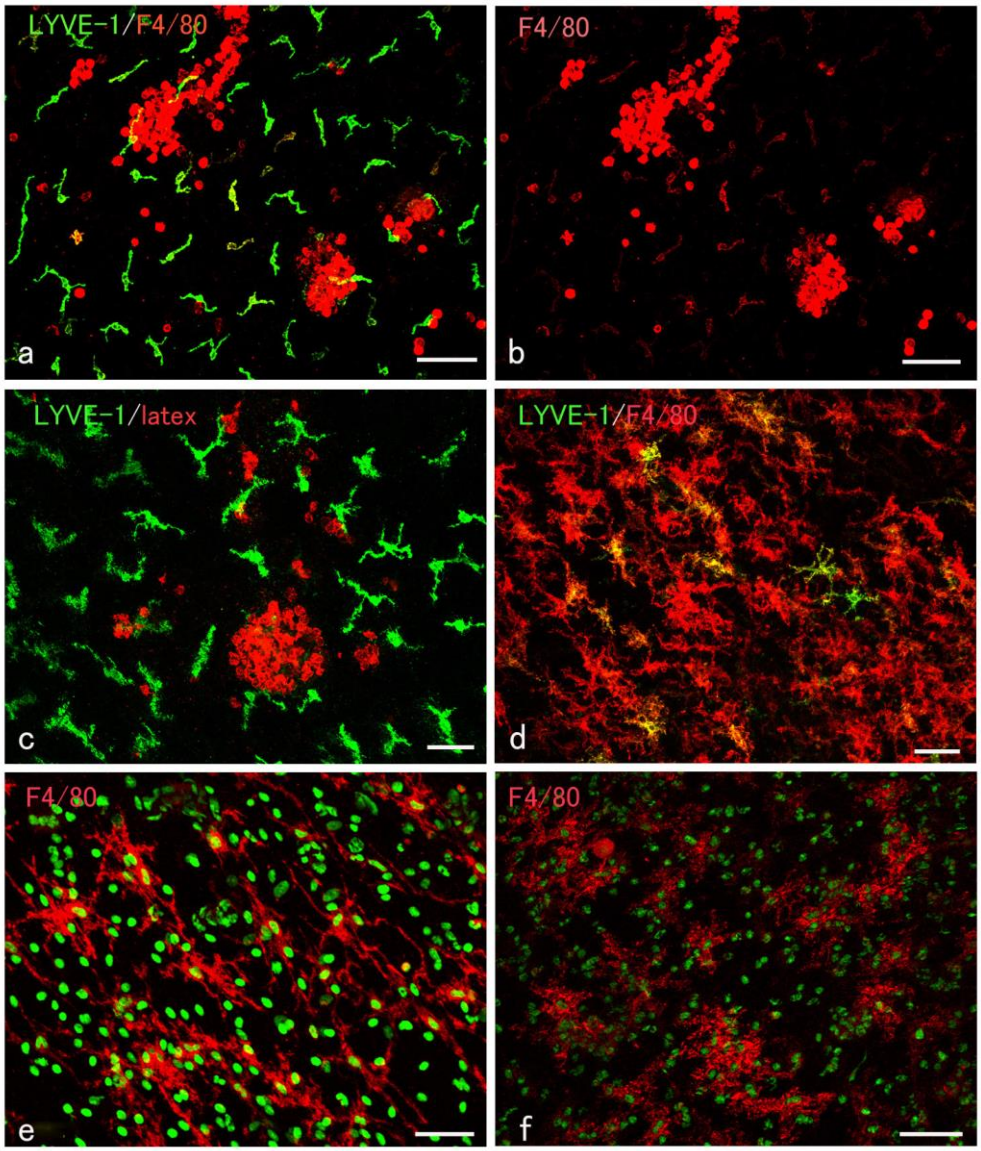

Fig. 9 Several characteristics of LYVE-1$^+$ cells in the mesentery. Double staining for LYVE-1 (green) and F4/80 (red) demonstrates that LYVE-1$^+$ cells are weakly positive for F4/80, while F4/80$^+$ round macrophages are absolutely negative for LYVE-1 (a, b). When latex beads of 20 nm in diameter were injected into the peritoneal cavity, only round cells (macrophages) ingested the latex bead 3 h after injection (c). When LPS was injected, LYVE-1$^+$ cells (green) decreased in number, indicating a severe loss of LIVE-1 immunoreactivity 2 days after injection, while the immunoreactivity for F4/80 increased in intensity (d). Two days after injection of LPS, Type 1 cells with dendritic morphology, now visible by F4/80 antibody, extended longer processes, like astrocytes (e). Type 2 cells also changed in morphology (f). In figures e and f, nuclei are stained green by SyTO green. Bars: 100 μm (a, b), 50 μm (c–f)

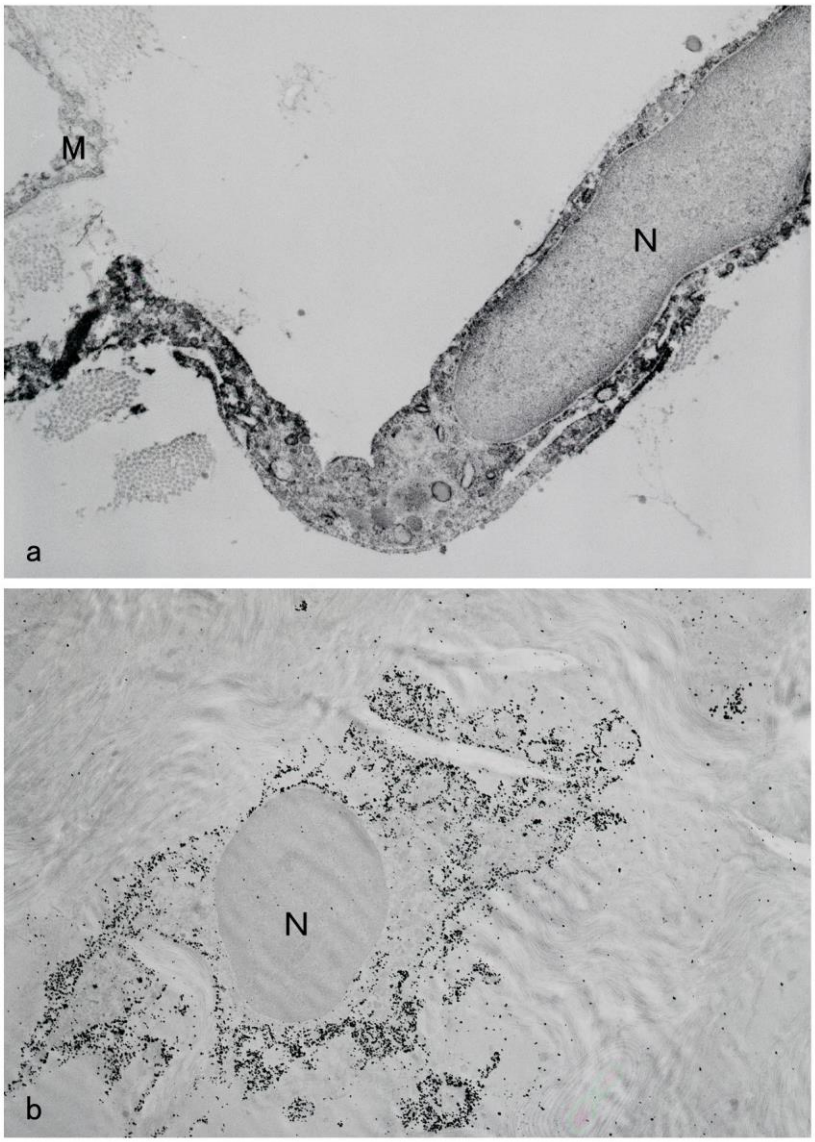

Fig. 10 Electron microscopy of LYVE-1-immunoreactive cells. Positive reactivity for LYVE-1 appears as a black deposit (a). The cytoplasm contains rough endoplasmic reticulum and vesicles of various sizes. In b, a LYVE-1 immunoreactive cell is seen in a horizontal plane of the mesentery. Immunogold particles for LYVE-1 are localized mainly along the plasma membrane of a dendritic cell, which is surrounded by collagen fibrils. M: mesothelium, N: nucleus

macrophages dispersed in the pia mater stained positively for LYVE-1 (Fig. 11b). The ovary contained numerous F4/80^{+} macrophages—especially rich in the corpus luteum, but again these macrophages were immunonegative for LYVE-1 (Fig. 11c). Hepatic sinusoidsal macrophages (Kupffer cells), alveolar macrophages, and macrophages numerous in the medulla of the lymph node and red pulp of the spleen were all negative for LYVE-1. F4/80^{+} macrophages occupying the lamina propria of the small intestine were also immunonegative for LYVE-1 (Fig. 11d). The LYVE-1-immunonegative macrophages mentioned above are regarded as resident and non-fixed macrophages which are not embedded in the connective tissues.

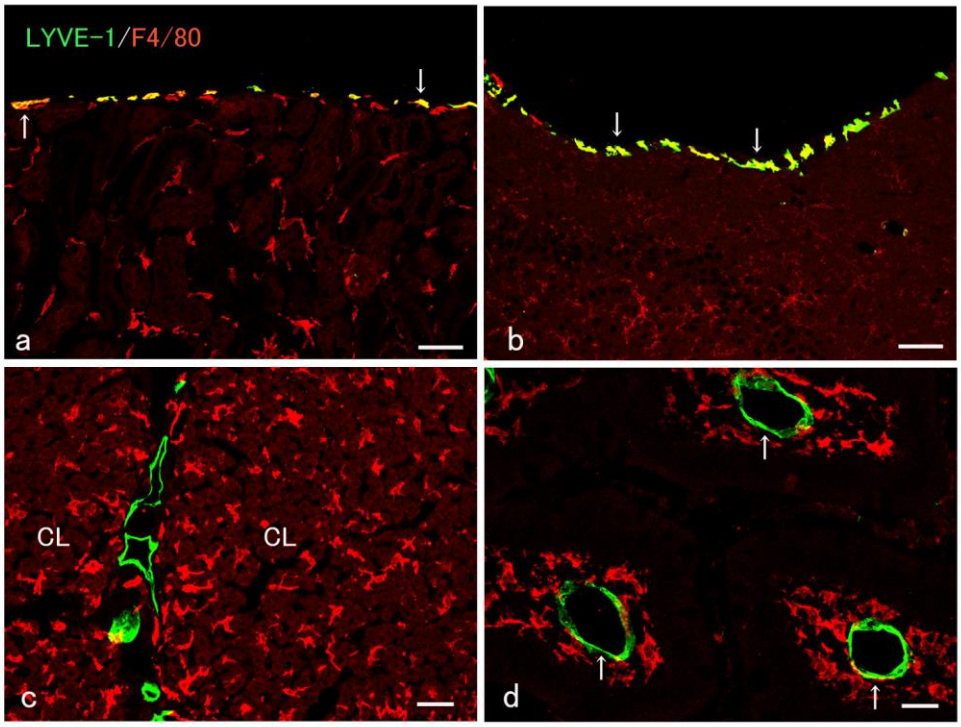

Fig. 11 Double immunostaining of LYVE-1 and F4/80 in macrophages of various tissues. In the kidney (a) and brain (b), LYVE-1 immunoreactivity is found only in macrophages dispersed in a capsule of the kidney (a) and pia mater of the brain (b), as indicated by arrows. F4/80^{+} macrophages are numerous in the corpus luteum (CL in **c**) and lamina propria of intestinal villi (d) but free from any immunoreactivity for LYVE-1. In figure **d**, three intestinal villi have been obliquely cut where lymphatic vessels are selectively positive green for LYVE-1 (arrows). Bras: 50 μm (a, b), 20 μm (c, d)

Discussion

LYVE-1-immunoreactive macrophages embedded in connective tissues

Several types of macrophages share the LYVE-1 molecule with lymphatic endothelial cells. LYVE-1 is expressed in typical $CD11b^+$ $F4/80^+$ macrophages are dispersed in connective tissues around tumors and in wound healing tissues[78]. Fetal macrophages in the human placenta and murine kidney are also LYVE-1-immunoreactive[51,79], though macrophages in the kidney of adult mice lose this immunoreactivity[51]. The present study revealed a broad distribution of LYVE-1^+ macrophages in adult animals under normal conditions. LYVE-1-immunoreactive $F4/80^+$ macrophages were dispersed in various connective tissues of the visceral organs, such as the capsule and interstitium of the kidney, thymus, lymph node, and brown adipose tissue. However, none of the $F4/80^+$ macrophages present in the parenchyma of the kidney, thymus, or brain expressed LYVE-1. This lack of LYVE-1 expression was consistent in macrophages residing in hepatic sinusoids, pulmonary alveoli, medulla of the lymph node, and red pulp of the spleen. These LYVE-1-negative macrophages are not embedded in the connective tissue and may lack an intimate relation to the extracellular matrix. It is hard to conclude that LYVE-1^- macrophages in the lamina propria of intestinal villi are embedded in the collagen-rich connective tissue. Collectively, only macrophages anchored in the connective tissue tend to express the hyaluronan-binding molecule, LYVE-1. Hyaluronan is ubiquitously and most abundantly present in the extracellular matrix of tissues where it interacts with numerous proteins to form a hygroscopic matrix important for cell adhesion and migration. Thus, it is likely that LYVE-1 plays a role in the formation of scaffolds of macrophages for cell adhesion to the extracellular matrix.

LYVE-1^+ macrophagic cells in the mesentery

Macrophages with dendritic morphology in the omentum of mice were F4/80- and Ia antigen-positive and showed a spindle, dendritic, or stellate shape[75]. The number of omental macrophages was severely reduced in *op/op* mice, which were genetically

deficient in a macrophage lineage[75]. Similarly, ED2-positive spindle-shaped macrophages in the rat omentum were completely eliminated by the uptake of liposome-encapsulated clodronate, a toxic substance[80]. Those cells with dendritic morphology in the murine omentum were negative for markers for Langerhans/dendritic cells[75], in agreement with the lack of immunoreactivity for CD11c in the present study. These findings suggest that the cells in question are macrophagic in origin rather than Langerhans/dendritic/interdigitating cells. However, our cells in the murine mesentery differed in both shape and immunoreactivity to F4/80 and LYVE-1 antibodies from typical macrophages. The F4/80-intensely positive macrophages of the mesentery are round in shape, negative for LYVE-1, and exposed to the peritoneal cavity. Since the F4/80$^+$ round cells only can vigorously ingest foreign bodies like latex particles, they function as typical scavenger macrophages. The phagocytic activity of omental dendritic cells is very low 3 h after an intraperitoneal injection of colloidal carbons, but one day after administration, they actively ingested carbon particles[75]. We also found that mesenteric LYVE-1$^+$ cells can ingest latex particles to some degree one day after injection. This suppressed ability to ingest foreign particles may be due to their being embedded in membranous tissues.

When considering the classification of mesenteric dendritic cells, their response to LPS becomes important. In the murine mesentery, LYVE-1$^+$ cells with dendritic processes (Type 1 and Type 2 cells) were weakly positive for F4/80. The F4/80 immunoreactivity of LYVE-1$^+$ cells increased in intensity by LPS stimulation together with a dynamic morphologic change, indicating that they quickly respond to inflammatory events. It remains unsettled as to whether the LYVE-1$^+$ cells are precursors of F4/80$^+$ round macrophages (and peritoneal macrophages) or macrophages of a special subtype different from typical macrophages. The LYVE-1$^+$ macrophage-like cells in the mesentery showed a quite even, characteristic distribution and their processes were well arranged with a regular direction and intercellular gaps. This characteristic regular arrangement is shared by other macrophages: for example, brain macrophages (microglia) are evenly distributed throughout the brain under normal conditions. At the present time,

the LYVE-1$^+$ macrophage-like cells in the mesentery should be classified as a kind of tissue type of macrophage.

The existence of Type 2 LYVE-1$^+$ cells in the murine mesentery has not been documented yet. It is worth noting that this type of cell was also evenly distributed and its distribution supplemented the distribution of Type 1 LYVE-1$^+$ cells. Although weakly positive for F4/80 under normal conditions, the immunoreactivity to F4/80 increased in intensity in response to LPS attack, as did Type 1 LYVE-1$^+$ cells. Further study is needed to reveal their exact relationship.

Involvement of LYVE-1$^+$ cells in inflammation

It was remarkable that the mesenteric dendritic cells almost lost their LYVE-1 immunoreactivity as well as undergoing morphological changes by an LPS challenge, demonstrating their sharp responsiveness to an inflammatory environment. We confirmed similar changes in mesenteric dendritic cells with a peritoneal injection of Freund' adjuvant (our unpublished data). These changes compare with the finding that pro-inflammatory cytokines such as TNFα□ □□□□□□ a rapid internalization of LYVE-1 in lymphatic endothelial cells followed by terminal degradation in lysosomes[60]. Another down-regulation of the hyaluronan receptor was noted in lymphatic vessels during the early stages 24–48 h after mycoplasma infection[60]. LYVE-1 is also lost from hepatic sinusoidal endothelial cells during inflammation[42] and from lymphatic vessels in the early phase of some murine models accompanied with muscle degeneration and inflammation, possibly due to the induction of TNFα□□. On the other hand, high molecular weight hyaluronan modulates inflammatory responses in macrophages: it inhibits LPS-induced inflammatory signalings in macrophages and microglia[82–85]. This action was explained by the interaction of hyaluronan with another hyaluronan receptor, CD44, which shares 41% homology with LYVE-1[83]. Although any direct interaction of hyaluronan with LYVE-1 is unknown, the loss of LYVE-1 in macrophagic cells of the mesentery may be involved in the activation of inflammatory responses. In fact, Wardrop and Dominov[81]

described how the disappearance of LYVE-1 in lymphatic vessels provides a sensitive biomarker to monitor active inflammatory or tissue damages.

In conclusion, LYVE-1 is a powerful marker to study the morphology and functional significance of the cells with dendritic morphology in the mesentery. Their characteristic morphology and quick response to a LPS challenge shown by the present study suggest their important roles in the maintenance of the peritoneal cavity and organs.

Conclusion

LYVE-1, a receptor molecule for hyaluronan, is expressed in the lymphatic endothelium, blood sinus endothelium, and certain macrophage lineages. The present immunohistochemical study using an anti-LYVE-1 antibody obtained the following results.

1. LYVE-1 showed a broader distribution of LYVE-1 in vascular endothelial cells of the murine lung, adrenal gland, and heart as well as the liver and spleen. In addition, sinus reticular cells in the medulla of the lymph node also intensely expressed LYVE-1. Ultrastructurally, immuno-gold particles for LYVE-1 were localized on the entire length of plasma membrane in all cell types.
2. An LPS stimulation elevated the expression at mRNA and protein levels of LYVE-1 in the liver and lung, major organs for the elimination of blood-born waste substances. LYVE-1-expressing endothelial cells in these organs participated in the endocytosis of exogenous particles, and the uptake ability was conspicuously enhanced by the LPS challenge.
3. Although the expression of hyaluronidases was generally low in the LYVE-1-expressing cells, they were topographically associated with a dense distribution of macrophages possessing hyaluronidase activities in each tissue.
4. Under normal conditions, F4/80^{+} macrophages embedded in connective tissues expressed LYVE-1, in contrast to lack of LYVE-1 in F4/80^{+} macrophages within the parenchyma of visceral organs and those freely residing in hepatic sinusoids and pulmonary alveoli.
5. Immunostaining using whole mount preparations of the murine mesentery revealed two novel types of LYVE-1-immunoreactive cells with dendritic morphology other than F4/80^{+} typical macrophages. They were regularly distributed with constant intervals throughout the mesentery and appeared to possess their own territory. Both types of LYVE-1^{+} cells were weakly or moderately immunopositive for F4/80, while F4/80^{+} round macrophages were absolutely free from the LYVE-1 immunoreactivity. Only macrophages could ingest latex particles after a peritoneal injection.

6. Peritoneal administration of LPS induced a rapid reduction of LYVE-1 immunoreactivity in the cells with dendritic morphology followed by an increased immunoreactivity to F4/80 antibody, and simultaneously by dynamic changes in their shape.

LYVE-1 may be a reliable marker of the reticulo-endothelial system (RES) specialized for eliminating foreign particles. Furthermore, the LYVE-1-expressing RES cells might be involved in the uptake of hyaluronan and other waste products as well as foreign particles circulating in the blood and lymph while participating in the subsequent degradation in relay with adjacent macrophage populations. Macrophages belong to the RES and some macrophage lineages express LYVE-1. LYVE-1 may play a role in cell adhesion and migration of macrophagic cells within connective tissues rich in hyaluronan, and loss of LYVE-1 becomes a reliable sign of activated conditions in inflammation. LYVE-1 expression in macrophagic cells may give new insights in classification and functional consideration of macrophages.

Acknowledgements

The research summarized in this thesis has been carried out at the Laboratory of Histology, Graduate school of Medical school, Hokkaido University during the years 2012–2016 under the Ph.D. course.

First and foremost, I would like to express my deepest gratitude to my supervisor Professor Iwanaga Toshihiko for giving me the opportunity to study in this lab. It is my honor to be his student. Without him consistent trust and encouragement, I could not start and complete my doctoral career in the best and most beautiful palace—Hokkaido University. I usually made many mistakes during the process of experiments or paper-wring, without blaming and giving up, Professor Iwanaga consisted to extremely generous with his time to instructed me. Not only offered me any recourses what I need during the experiments, but also lots of valuable suggestions when he reviewed my manuscripts. He is the one who taught me how to organize a story logically in order to accentuate the key points of our research, which is significant for a doctor student to understand how to design the experiments to testify the scientific hypothesis.

I also want to express my sincere gratitude to Professor Iwanaga Hiromi. She is the one who makes me feel the lab more like a family. Her caring and encourage every day is my energy resource.

Doctor Kobayashi Junko, although she is not my supervisor, she offered me help whenever and whatever I need. She is there for each important moment: the first oral presentation, the first poster, all the rehearsals, every tears and congratulations. She is the one who not only makes me become a better student, but also a better person.

I also want to thank Doctors Kimura Shunsuke and Kimura Megumi. They helped me not only the experiments but also my personal life. Thank you so much for caring about me and helping me.

All the members in the lab of Histology of Hokkaido University have contributed immensely to my personal and professional time in Sapporo. They are a good source of friendships in my daily life and good advice and collaboration in the experiments and seminars. Thank you all for accompany me in the past four years.

Thank you for the mice which sacrificed during research.

Thanks a lot to Hokkaido University for giving me the tuition fees exemption, the OTOWA HIROTSUGU scholarship for giving me the foundation, the Top Global

University Project for giving me the foundation, and the Japanese Government for giving me the foundation.

Great acknowledgement is given to my parents and brother Yang for all their love, understanding and encouragement throughout my life.

At last, special appreciation is expressed to my friends in Sapporo. Almost all my spare time were occupied by Qingnan Chu, Fuqing Xie, Chengbo Tan, Wang Yi, Mohan, Iwazumi Aki, Takemoto Konomi and so on. It is my honor and lucky to spend time and make good memories with them. Thank you to everyone for being there every time when I need. You guys are the colorful elements in my life.

References

1. Fraser, J. R., Laurent, T. C. & Laurent, U. B. Hyaluronan: its nature, distribution, functions and turnover. *J. Intern. Med.* **242**, 27–33 (1997).
2. Toole, B. P. Hyaluronan: from extracellular glue to pericellular cue. *Nat. Rev. Cancer* **4**, 528–539 (2004).
3. Prehm, P. Hyaluronate is synthesized at plasma membranes. *Biochem. J.* **220**, 597–600 (1984).
4. Itano, N. & Kimata, K. Mammalian hyaluronan synthases. *IUBMB Life* **54**, 195–199 (2002).
5. Weigel, P. H. Functional characteristics and catalytic mechanisms of the bacterial hyaluronan synthases. *IUBMB Life* **54**, 201–211 (2002).
6. Itano, N., et al. (1999) Three isoforms of mammalian hyaluronan synthases have distinct enzymatic properties. *J. Biol. Chem.* **274**, 25085–25092 (1999).
7. Chang, M. Y., et al. A rapid increase in macrophage-derived versican and hyaluronan in infectious lung disease. *Martix Biol.* **34**, 1–12 (2014).
8. Horton, M. R., et al. Hyaluronan fragments synergize with interferon-gamma to induce the C-X-C chemokines mig and interferon-inducible protein-10 in mouse macrophages. *J. Biol. Chem.* **273**, 35088–35094 (1998).
9. McKee, C. M., et al. Hyaluronan fragments induce nitric-oxide synthase in murine macrophages through a nuclear factor kappaB-dependent mechanism. *J. Biol. Chem.* **272**, 8013–8018 (1997).
10. McKee, C. M., et al. Hyaluronan (HA) fragments induce chemokine gene expression in alveolar macrophages. The role of HA size and CD44. *J. Clin. Invest.* **98**, 2403–2413 (1996).
11. Noble, P. W., McKee, C. M., Cowman, M. & Shin, H. S. Hyaluronan fragments activate an NF-kappa B/I-kappa B alpha autoregulatory loop in murine macrophages. *J. Exp. Med.* **183**, 2373–2378 (1996).
12. Termeer, C. C., et al. Oligosaccharides of hyaluronan are potent activators of dendritic cells. *J. Immunol.* **165**, 1863–1870 (2000).
13. Jiang, D., Liang, J. & Noble, P. W. Hyaluronan as an immune regulator in human diseases. *Physiol. Rev.* **91**, 221–264 (2011).

14. Lepperdinger, G., Strobl, B. & Kreil, G. HYAL2, a human gene expressed in many cells, encodes a lysosomal hyaluronidase with a novel type of specificity. *J. Biol. Chem.* **273**, 22466–22470 (1998).
15. Chajara, A., et al. Increased hyaluronan and hyaluronidase production and hyaluronan degradation in injured aorta of insulin-resistant rats. *Arterioscler. Thromb. Vasc. Biol*. **20**, 1480–1487 (2000).
16. Fraser, J.R. & Laurent, T. C. Turnover and metabolism of hyaluronan. *Ciba Found. Symp.* **143**, 41–53 (1989).
17. Laurent, T. C. & Fraser, J. R. Hyaluronan. *FASEB J.* **6**, 2397–2404 (1992).
18. Hickey, M. J. & Kubes, P. Intravascular immunity: the host–pathogen encounter in blood vessels. *Nat. Rev. Immunol*. **9**, 364–375 (2009).
19. Harris, E. N., Weigel, J. A. & Weigel, P. H. The human hyaluronan receptor for endocytosis (HARE/Stabilin-2) is a systemic clearance receptor for heparin. *J. Biol. Chem.* **283**, 17341–17350 (2008).
20. Aruffo, A., et al. CD44 is the principal cell surface receptor for hyaluronate. *Cell* **61**, 1303–1313 (1990).
21. Sherman, L., Sleeman, J., Herrlich, P. & Ponta, H. Hyaluronate receptors: key players in growth, differentiation, migration and tumor progression. *Curr. Opin. Cell Biol.* **6**, 726–733 (1994).
22. Pandey, M. S. & Weigel, P. H. A hyaluronan receptor for endocytosis (HARE) link domain N-glycan is required for extracellular signal-regulated kinase (ERK) and nuclear factor-κB (NF-κB) signaling in response to the uptake of hyaluronan but not heparin, dermatan sulfate, or acetylated low density lipoprotein (LDL). *J. Biol. Chem.* **289**, 21807–21817 (2014).
23. Zhou, B., Weigel, J. A., Saxena A. & Weigel, P. H. Molecular cloning and functional expression of the rat 175-kDa hyaluronan receptor for endocytosis. *Mol. Biol. Cell* **13**, 2853–2868 (2002).
24. Laurent, U. B. & Reed, R. K. Turnover of hyaluronan in the tissues. *Advan. Drug Deliv. Rev.* **7**, 237–256 (1991).

25. Chen, W. Y. & Abatangelo, G. Functions of hyaluronan in wound repair. *Wound Repair Regen.* **7**, 79–89 (1999).
26. Hardwick, C., et al. Molecular cloning of a novel hyaluronan receptor that mediates tumor cell motility. *J. Cell. Biol.* **117**, 1343–1350 (1992).
27. Yang, B., Zhang, L. & Turley, E. A. Identification of two hyaluronan-binding domains in the hyaluronan receptor RHAMM. *J. Biol. Chem.* **268**, 8617–8623 (1993).
28. Misra, S., Hascall, V. C., Markwald, R. R. & Ghatak, S. Interactions between hyaluronan and its receptors (CD44, RHAMM) regulate the activities of inflammation and cancer. *Front. Immunol.* **6**, 201 (2015).
29. Rizzardi, A. E., et al. Elevated hyaluronan and hyaluronan-mediated motility receptor are associated with biochemical failure in patients with intermediate-grade prostate tumors. *Cancer* **120**, 1800–1809 (2014).
30. Banerji, S., et al. LYVE-1, a new homologue of the CD44 glycoprotein, is a lymph-specific receptor for hyaluronan. *J. Cell. Biol.* **144**, 789–801 (1999).
31. Jackson, D. G. Biology of the lymphatic marker LYVE-1 and applications in research into lymphatic trafficking and lymphangiogenesis. *APMIS* **112**, 526–538 (2004).
32. Mouta Carreira, C., et al. LIVE-1 is not restricted to the lymph vessels: expression in normal liver blood sinusoids and down-regulation in human liver cancer and cirrhosis. *Cancer Res.* **61**, 8079–8084 (2001).
33. Aschoff, L. Reticuloendothelial System (Janeway Lecture, New York). Lectures on Pathology (delivered in the United States, 1924). Paul B. Hoeber, Inc., pp. 1–33, New York.
34. Van Furth, R., et al. The mononuclear phagocyte system: a new classification of macrophages, monocytes and their precursor cells. *Bull. World Health Organ* **46**, 845–852 (1972).
35. Kawai, Y., Smedsrød, B., Elvevold, K. & Wake, K. Uptake of lithium carmine by sinusoidal endothelial and Kupffer cells of the rat liver: new insights into the classical vital staining and the reticulo-endothelial system. *Cell Tissue Res.* **292**, 395–410 (1998).
36. Smedsrød, B., Pertoft, H., Gustafson, S. & Laurent, T. C. Scavenger functions of the liver endothelial cell. *Biochem. J.* **266**, 313–327 (1990).

37. Delves, P. J., Martin, S. J., Burton, D. R. & Roit, I. M. *Roitt's Essential Immunology* (11th ed.). Blackwell Publishing, Malden, MA, 2006.
38. Daems, W. T. & Brederro, P. The fine structure and peroxidase activity of resident and exudate macrophages in the guinea pigs. In: The Reticuloendothelial System in Health and Disease (Reichard, S. M., Escobar, M. R. & Fiedman, H., eds.). *Adv. Exp. Med. Biol.* **73A**, 27–40 (1976).
39. Oh, J., et al. Endoplasmic reticulum stress controls M2 macrophage differentiation and foam cell formation. *J. Biol. Chem.* **287**, 11629–11641 (2012).
40. Prevo, R., et al. Mouse LYVE-1 is an endocytic receptor for hyaluronan in lymphatic endothelium. *J. Biol. Chem.* **276**, 19420–19430 (2001).
41. Lesley, J., Hyman, R. & Kincade, P. W. CD44 and its interaction with the extracellular matrix. *Adv. Immunol.* **54**, 271–335 (1994).
42. Akishima, Y., et al. Immunohistochemical detection of human small lymphatic vessels under normal and pathological conditions using the LYVE-1 antibody. *Virchows Arch.* **444**, 153–157 (2004).
43. Aschoff, L. Das reticulo-endotheliale System. *Ergebn. Inn. Med. Kinderheilk.* **26**, 1–118 (1924).
44. Sørensen, K. K., Simon-Santamaria, J., McCuskey, R.S. & Smedsrød, B. Liver sinusoidal endothelial cells. *Compr. Physiol.* **5**, 1751–1774 (2015).
45. Sørensen, K. K., et al. The scavenger endothelial cell: a new player in homeostasis and immunity. *Am. J. Physiol. Gastrointest. Liver Physiol.* **301**, G1217–1230 (2012).
46. Wake, K., Kawai, Y. & Smedsrød, B. Re-evaluation of the reticulo-endothelial system. *It. J. Anat. Embryol.* **106** (Suppl 1), 261–269 (2001).
47. Rung-ruangkijkrai, T., et al. The expression of *src*-suppressed C kinase substrate (SSeCKS) and uptake of exogenous particles in endothelial and reticular cells. *Arch. Histol. Cytol.* **67**, 135–147 (2004).
48. Kitamura, H., et al. Induction of Src-suppressed C kinase substrate (SSeCKS) in vascular endothelial cells by bacterial lipopolysaccharide. *J. Histochem. Cytochem.* **50**, 245–255 (2002).

49. Jiang, D., Liang, J. & Noble, P.W. Hyaluronan as an immune regulator in human diseases. *Physiol. Rev.* **91**, 221–264 (2011).
50. Arimoto, J., et al. Expression of LYVE-1 in sinusoidal endothelium is reduced in chronically inflamed human livers. *J. Gastroenterol.* **45**, 317–325 (2010).
51. Lee, H., et al. Expression of lymphatic endothelium-specific hyaluronan receptor LYVE-1 in the developing mouse kidney. *Cell Tissue Res.* **343**, 429–444 (2011).
52. Zheng, M., et al. Three types of macrophagic cells in the mesentery of mice with special reference to LYVE-1-immunoreactive cells. *Biomed. Res. (Tokyo)* **35,** 37–45 (2014).
53. Gordon, E. J., Gale, N. W. & Harvey, N. L. Expression of the hyaluronan receptor LYVE-1 is not restricted to the lymphatic vasculature; LYVE-1 is also expressed on embryonic blood vessels. *Dev. Dyn.* **237**, 1901–1909 (2008).
54. Altura, B. M. Reticuloendothelial cells and host defense. *Adv. Microcirc.* **9**, 252–294 (1980).
55. McCourt, P.A., Smedsrød, B. H., Melkko, J. & Johansson, S. Characterization of a hyaluronan receptor on rat sinusoidal liver endothelial cells and its functional relationship to scavenger receptors. *Hepatology* **30**, 1276–1286 (1999).
56. Politz, O., et al. Stabilin-1 and stabilin-2 constitute a novel family of fasciclin-like hyaluronan receptor homologues. *Biochem. J.* **362**, 155–164 (2002).
57. Falkowski, M., Schledzewski, K., Hansen, B. & Goerdt, S. Expression of stabilin-2, a novel fasciclin-like hyaluronan receptor protein, in murine sinusoidal endothelia, avascular tissues, and at solid/liquid interfaces. *Histochem. Cell Biol.* **120**, 361–369 (2003).
58. Gale, N. W., et al. Normal lymphatic development and function in mice deficient for the lymphatic hyaluronan receptor LYVE-1. *Mol. Cell Biol.* **27**, 595–604 (2007).
59. Nightingale, T.D., et al. A mechanism of sialylation functionally silences the hyaluronan receptor LYVE-1 in lymphatic endotheium. *J. Biol. Chem.* **284**, 3935–3945 (2009).
60. Johnson, L.A., Prevo, R., Clasper, S. & Jackson, D. G. Inflammation-induced up take and degradation of the lymphatic endothelial hyaluronan receptor LYVE-1. *J. Biol. Chem.* **282**, 33671–33680 (2007).
61. Maiolino, S., et al. Hyaluronan-decorated polymer nanoparticles targeting the CD44 receptor

for the combined photo-chemo-therapy of cancer. *Nanoscale* **7**, 5643–5653 (2015).

62. Song, S., et al. (2014) Hyaluronan-based nanocarriers with CD44-overexpressed cancer cell targeting. *Pharm. Res.* **31**, 2988–3005 (2014).
63. Cai, S., et al. Cellular uptake and internalization of hyaluronan-based doxorubicin and cisplatic conjugates. *J. Drug. Target.* **22**, 648–657 (2014).
64. Bumbasirevic, V., Pappas, G. D. & Becker, R.P. Endocytosis of serum albumin-gold conjugates by microvascular endothelial cells in rat adrenal gland: regional differences between cortex and medulla. *J. Submicrosc. Cytol. Pathol.* **22**, 135–145 (1990).
65. Yedgar, S., et al. Tissue sites of catabolism of albumin in rabbits. *Am. J. Physiol.* **244**, E101–E107 (1983).
66. Florey, L. The uptake of particulate matter by endothelial cells. *Proc. R. Soc. Lond B Biol. Sci.* **166**, 375–383 (1967).
67. Qian, H., et al. (2009) Stabilins are expressed in bone marrow sinusoidal endothelial cells and mediate scavenging and cell adhesive functions. *Biochem. Biophys. Res. Commun.* **390**, 883–886 (2009).
68. Smedsrød, B., Olsen, R. & Sveinbjørnsson, B. Circulating collagen is catabolized by endocytosis mainly by endothelial cells of endocardium in cod (*Gadus morhua*). *Cell Tissue Res.* **280**, 39–48 (1995).
69. Sørensen, K. K., Dahl, L. B. & Smedsrød, B. (1997) Role of endocardial endothelial cells in the turnover of hyaluronan in Atlantic cod (*Gadus morhua*). *Cell Tissue Res.* **290**, 101–109 (1997).
70. Fraser, J. R. & Laurent, T. C. Turnover and metabolism of hyaluronan. *Ciba Found. Symp.* **143**, 41–53 (1989).
71. Laurent, T. C. & Fraser, J. R. Hyaluronan. *FASEB J.* **6**, 2397–2404 (1992).
72. Harris, E.N., Weigel, J. A. & Weugel, P. H. The human hyaluronan receptor for endocytosis (HARE/stabilin-2) is a systemic clearance receptor for heparin. *J. Biol. Chem.* **283**, 17341–17350 (2008).
73. Fujita, H. & Kataoka, K. Capillary endothelial cells of the anterior pituitary should be excluded

from the reticulo-endothelial system. *Z. Anat. Entwickl-Gesch.* **128**, 318–328 (1969).

74. Holub, M., et al. Omental dendritic cells: Ia expression and relation to macrophages. *APMIS* **98**, 1113–1122 (1990).
75. Zhu, H., et al. Macrophage differentiation and expression of macrophage colony-stimulating factor in murine milky spots and omentum after macrophage elimination. *J. Leukoc. Biol.* **61**, 436–444 (1997).
76. Fraser, J. R. E., et al. Uptake and degradation of hyaluronan in lymphatic tissue. *Biochem. J.* **256**, 153–158 (1988).
77. Grant, A. J., et al. Hepatic expression of secondary lymphoid chemokine (CCL21) promotes the development of portal-associated lymphoid tissue in chronic inflammatory liver disease. *Am. J. Pathol.* **160**, 1445–1455 (2001).
78. Schledzewski, K., et al. Lympahtic endothelium-specific hyaluronan receptor LYVE-1 is expressed by stabilin-1^+, F4/80^+, $CD11b^+$ macrophages in malignant tumours and wound healing tissue *in vivo* and in bone marrow cultures *in vitro*: implications for the assessment of lymphangiogenesis. *J. Pathol.* **209**, 67–77 (2006).
79. Böckle, B. C., et al. DC-$SIGN^+$ $CD163^+$ macrophages expressing hyaluronan receptor LYVE-1 are located within chorion villi of the placenta. *Placenta* **29**, 187–192 (2008).
80. Biewenga, J., et al. Macrophage depletion in the rat after intraperitoneal administration of liposome-encapsulated clodronate: depletion kinetics and accelerated repopulation of peritoneal and omental macrophages by administration of Freund's adjuvant. *Cell Tissue Res.* **280**, 189–196 (1995).
81. Wardrop, K. E. & Dominov, J. A. Proinflammatory signals and the loss of lymphatic vessel hyaluronan receptor-1 (LYVE-1) in the early pathogenesis of laminin alpha2-deficient skeletal muscle. *J. Histochem. Cytochem.* **59**, 167–179 (2011).
82. Austin, J. W., Gilchrist, C. & Fehlings, M. G. High molecular weight hyaluronan reduces lipopolysaccharide mediated microglial activation. *J. Neurochem.* **122**, 344–355 (2012).
83. Muto, J., Yamasaki, K., Taylor, K. R. & Gallo, R. L. Engagement of CD44 by hyaluronan suppresses TRL4 signaling and the septic response to LPS. *Mol. Immunol.* **47**, 449–4565

(2009).

84. Yasuda, T. Hyaluronan inhibits cytokine production by lipopolysaccharide-stimulated U937 macrophages through down-regulation of NF-kappaB via ICAM-1. *Inflamm. Res.* **56**, 246–253 (2007).
85. Yasuda, T. Hyaluronan inhibits prostaglandin E2 production via CD44 in U937 human macrophages. *Tohoku J. Exp. Med.* **220**, 229–235 (2010).